



Strålsäkerhetsmyndigheten

Swedish Radiation Safety Authority

Authors:

Sitakanta Mohanty
Osvaldo Pensado

Technical Note

2014:33

Reproduction of SKB's Canister Failure Calculations

—What-If and 'Residual' Scenario to Illustrate Barrier Functions

Main Review Phase

SSM perspektiv

Bakgrund

Strålsäkerhetsmyndigheten (SSM) granskar Svensk Kärnbränslehantering AB:s (SKB) ansökningar enligt lagen (1984:3) om kärnteknisk verksamhet om uppförande, innehav och drift av ett slutförvar för använt kärnbränsle och av en inkapslingsanläggning. Som en del i granskningen ger SSM konsulter uppdrag för att inhämta information och göra expertbedömningar i avgränsade frågor. I SSM:s Technical note-serie rapporteras resultaten från dessa konsultuppdrag.

Projektets syfte

Det övergripande syftet med projektet är att ta fram synpunkter på SKB:s säkerhetsanalys SR-Site för den långsiktiga strålsäkerheten hos det planerade slutförvaret i Forsmark. Det specifika syftet med projektet är att bedöma SKB:s kapselbrottsberäkningar genom reproduktion av de så kallade "what-if" fallen och "restscenarierna" för att belysa barriärernas funktion. Upprepningen av SKB:s beräkningar bör ge kunskaper om alla de antaganden, modellbeskrivningar och parametervärden som ligger bakom beräkningarna och ge underlag för SSM:s bedömning av SKB:s säkerhetsanalys.

Författarnas sammanfattning

I SR-Site rapporten analyserade SKB en rad scenarier. SKB grupperade dessa scenarier i huvud- och restscenarier. Huvudscenariot inkluderade ett troligt scenario (korrosionsfallet) och ett mindre troligt scenario (det seismicitetsinducerade skjubrottsfallet). I restscenariot ingår två osannolika scenarier; isostatlastscenariot och "growing pinhole failure"-scenariot. För varje scenario analyserade SKB ett referensfall och flera varianter (som skapas genom att ändra funktioner och processer, samt genom att försämra barriärkomponenter) som kallas "what-if"-fall som syftar till känslighetsanalys och analys av barriärsfunktionerna.

Syftet med arbetet som redovisas i denna Technical Note är att utvärdera SKB:s "what-if"-analys för att undersöka om det är möjligt att reproducera resultaten och för att identifiera eventuella brister genom att undersöka SKB:s modellering. Undersökningen baseras på vad som kan utläsas av SKB rapporter och genom vår egen oberoende modellering. För att uppfylla detta syfte utvecklade vi en enkel modell för ett referensfall och utvalda "what-if"-fall. De "what-if"-fall som vi valde innefattar (i) korrosionsscenario med initial advektion, (ii) korrosionsscenario med snabbare upplösning av använt kärnbränsle (SNF), (iii) "growing pinhole"-scenariot med flöde längs förvarstunnlarnas hjässa på grund av kompakterad återfyllning (crown space), och (iv) "growing pinhole"-scenariot med kortare avstånd till skärningen mellan spricka och tunnel. Det övergripande målet var att utveckla en förståelse för förvarssystemets beteende för att kunna hitta eventuella brister i SKB: modell och för att identifiera aspekter som inte har beaktats av SKB.

Våra översiktliga gransknings- och modelleringsstudier fann att SKB för det mesta tydligt anger om parametervärden eller modellantaganden är

pessimistiska eller hypotetiska. Generellt sett har SKB beskrivit sina modelleringsmetoder och beräkningar tillräckligt transparent för att de ska kunna återskapas. Men det är inte tydligt om ett systematiskt tillvägagångssätt använts för att uttömmande söka efter kombinationer av barriär- eller systemkomponenter för att utveckla "what-if" scenarier eller analyser av barriärsfunktioner. SKB skulle också bättre kunna förklara olika aspekter av ett givet "what-if"-scenario som leder till ett lägre eller ett obetydligt dosekvivalent utsläpp (DER). Dessutom bör vissa processer (t.ex. förhållandet mellan flödesvägarna Q1, Q2 och Q3, probabilistiska simuleringsparametrar såsom flux, transportmotstånd och vatten-transporttider samt löslighet för Ra) beskrivas mer fullständigt för att öka transparensen och därmed reproducerbarheten av modellresultaten.

Vår oberoende analys kunde återskapa resultaten för SKB:s referensfall för de fyra referensscenarierna och för de "what-if"-fall vi analyserade, med avvikelser inom en faktor fem för både deterministiska och probabilistiska fall. Vi analyserade två "what-if"-fall som inte var med i SKB:s lista. Vi fann emellertid att de beräknade DER värdena från dessa ytterligare fall inte var signifikant större än resultaten från de fall som redan hade behandlats av SKB. Det bör noteras att våra modeller konstruerades baserat på generella beskrivningar av SKB:s modeller, och att efterforskningar rörande detaljer och implementering av dessa endast har gjorts om det varit absolut nödvändigt. Det är sannolikt att skillnaderna mellan våra resultat och SKB:s kan bli mindre genom att utveckla en bättre förståelse för SKB:s användning av flödesfält och flödeskorrelationer i olika delar av systemet. Därutöver bör ett bredare spektrum av SKB:s "what-if" analyser reproduceras.

Projektinformation

Kontaktperson på SSM: Shulan Xu
Diarienummer ramavtal: SSM2011-4243
Diarienummer avrop: SSM2013-2539
Aktivitetsnummer: 3030012-4049

SSM perspective

Background

The Swedish Radiation Safety Authority (SSM) reviews the Swedish Nuclear Fuel Company's (SKB) applications under the Act on Nuclear Activities (SFS 1984:3) for the construction and operation of a repository for spent nuclear fuel and for an encapsulation facility. As part of the review, SSM commissions consultants to carry out work in order to obtain information and provide expert opinion on specific issues. The results from the consultants' tasks are reported in SSM's Technical Note series.

Objectives of the project

The general objective of the project is to provide review comments on SKB's postclosure safety analysis, SR-Site, for the proposed repository at Forsmark. The objective of this assignment is to assess SKB's canister failure calculations through reproduction of the so called "what if" cases and "residual" scenarios to illustrate "barrier functions". The reproduction should provide insight into all the assumptions, model descriptions and parameter values behind the calculations and give a basis for SSM's judgment on SKB's safety case.

Summary by the authors

The Swedish Nuclear Fuel and Waste Management Company (SKB) included analysis of a range of scenarios in its SR-Site report. SKB grouped these scenarios into two categories—main and residual. The main scenario included a likely scenario (corrosion failure) and a less probable scenario (seismicity-induced shear failure). The residual scenario included two unlikely scenarios—*isostatic-load* and *growing pinhole failures*. For each of the scenarios, SKB analysed a reference case and several variations (created by altering features and processes, and by degrading barrier components) referred to as 'what-if' analysis cases for sensitivity and barrier function analyses.

The objective of the work reported in this Technical Note is to evaluate SKB's what if analysis for reproducibility of results and identify any shortcomings by probing SKB's modelling approach, based on what can be inferred from SKB reports and through our independent modelling. To fulfil this objective, we developed a simple model for the reference cases and selected what-if scenario cases. The what-if scenario cases we considered include (i) corrosion scenario with initial advection, (ii) corrosion scenario with faster spent nuclear fuel (SNF) degradation, (iii) growing pinhole scenario with flow in the disposal tunnels' crown region, and (iv) growing pinhole scenario with shorter distance to the fracture–tunnel intersection. The overall goal was to develop an understanding of the repository system's behaviour, so that we will be able to find any potential shortcomings in the SKB model and identify aspects that may have not been considered by SKB.

Our limited review and modelling studies found that, for the most part, SKB has clearly stated where parameter values or model assumptions are

pessimistic or hypothetical. In general, SKB has described its modelling approach and computations sufficiently transparently for independent reproduction. But it is not clear if a systematic approach was taken that exhaustively searches for barrier or system-component combinations to develop what-if scenarios or barrier function analysis cases. SKB could also better explain various aspects of a given what-if scenario leading to a lower or inconsequential dose equivalent release (DER). In addition, some processes (e.g., the relationship between the Q1, Q2, and Q3 pathway flows; probabilistic simulation parameters such as fluxes, transport resistance parameters, and water travel times; and Ra solubility, etc.) should be described more completely to enhance transparency and hence reproducibility of model results.

Our independent analysis reproduced SKB's reference case results for the four reference scenarios and the what-if cases we analysed, within a factor of five for both deterministic and probabilistic cases. We analysed two what-if cases that were not in the SKB list. However, we found that the DERs from these additional cases were not significantly greater than the results of cases already considered by SKB. It should be noted that our models were constructed based on broad descriptions of the SKB models, seeking and implementing details only where strictly needed. It is likely that the differences between our results and SKB's can be reduced by developing a better understanding of SKB's use of the flow fields and flow correlations in different parts of the system. Also, a broader spectrum of what if analyses carried out by SKB should be investigated for reproducibility.

Project information

Contact person at SSM: Shulan Xu



Strålsäkerhetsmyndigheten

Swedish Radiation Safety Authority

Authors: Sitakanta Mohant and Osvaldo Pensado
Southwest Research Institute, San Antonio, Texas, United States

Technical Note 57

2014:33

Reproduction of SKB's Canister
Failure Calculations

—What-If and 'Residual' Scenario to
Illustrate Barrier Functions

Main Review Phase

Date: February, 2014

Report number: 2014:33 ISSN: 2000-0456

Available at www.stralsakerhetsmyndigheten.se

This report was commissioned by the Swedish Radiation Safety Authority (SSM). The conclusions and viewpoints presented in the report are those of the author(s) and do not necessarily coincide with those of SSM.

Contents

1. Introduction	2
2. SKB's presentation	3
2.1. General Description of SKB's Model for Release Calculations.....	3
2.2. Canister Failure Cases	5
2.2.1. Canister Failure by Corrosion.....	5
2.2.2. Canister Failure by Shear Load.....	6
2.2.3. Canister Failure by Isostatic Load	6
2.2.4. Canister Failure by Growing Pinhole	7
2.3. SKB's What-If Analysis Cases.....	8
2.4. Motivation for Consultant's assessment.....	9
2.4.1. General Description of the CNWRA Model	10
2.4.2. Setting up the Model.....	11
2.4.3. Confirmation of What-If Calculations	12
3. The Consultants' overall assessment	23
3.1. Motivation of the assessment	23
3.2. The Consultants' assessment	23
3.2.1. Assessment of the SKB Documentation	23
3.2.2. Assessment of calculations	24
3.2.3. Overall assessment of the approach.....	25
4. References.....	27

1. Introduction

This technical note documents results from an independent assessment of the Swedish Nuclear Fuel and Waste Management Company (SKB)'s computations documented in SKB's Radionuclide Transport Report for the Safety Assessment SR-Site (SKB, 2010a) and the SR-Site main report (SKB, 2011) for a variety of scenarios. The assessment involves testing the reproducibility of key scenario cases as well as "what if" cases as variants to key scenario calculations developed by SKB in SR-Site to assess risk significance, assess sensitivity, and to illustrate "barrier functions." The goal of this in-depth evaluation is to gain insights into whether the SKB radionuclide transport computations are appropriate to support the SKB conclusions on repository safety. The activities documented in this technical note are intended to support the Swedish Radiation Safety Authority's (SSM's) review activities of the SKB performance assessment computations.

In 2012, the reviewers at the Center for Nuclear Waste Regulatory Analyses (CNWRA[®]), Southwest Research Institute[®] (SwRI[®]) independently developed a simplified model of radionuclide transport to reproduce results for the "main" scenarios related to canister failure (i.e., corrosion canister failure scenario and shear load canister failure scenario) (Pensado and Mohanty, 2012). The associated review focused on a selected set of computations to evaluate the transparency in the SKB calculations.

For this technical note, the CNWRA reviewers extended the previously developed simplified model to add capabilities for analysing additional scenarios, especially residual scenarios (i.e., growing pinhole failure and isostatic load failure scenarios), to facilitate verification of what-if analyses SKB documented in support of SR-Site as well as new what-if analysis cases. Reviewing the adequacy and technical basis of the input data is beyond the scope of this activity.

Four SKB reports and accompanying appendices—TR-11-01, Long-term Safety for the Final Repository at Forsmark: Main Report of the SR-Site Project (SKB, 2011); TR-10-50, Radionuclide Transport Report for the Safety Assessment SR-Site (SKB, 2010), hereafter referred to simply as the "Radionuclide Transport Report;" TR-10-52, Data Report for the Safety Assessment SR Site (SKB, 2010a), hereafter referred to simply as the "Data Report;" R-09-20, Groundwater Flow Modelling of Periods with Temperate Climate Conditions-Forsmark (Joyce et al., 2010)—are the main sources of information and data in our verification computations. The reviewers have adopted first-person usage in this technical note to make a clear distinction between our verification computations and the SKB computations. We use terms such as "we computed" or "our computations" to clarify which modelling tasks have been performed as part of this review assignment, as opposed to the modelling that was performed by SKB.

2. SKB's presentation

SKB considers scenarios leading to canister failure and release of radionuclides from the spent nuclear fuel (SNF). We examined various SKB documents, including the license application (TR-11-01), and the radionuclide transport report (TR-10-50), to assess how the residual scenarios are modelled and how the what-if analyses are carried out by SKB to support safety analysis and barrier function analysis. In Section 2.1, we provide a general description of SKB's model, a summary of the SKB's failure scenarios, and a summary of the SKB's what-if scenarios. Section 2.1 is aimed at collecting main aspects of scenario modelling to facilitate comparison and understanding of differences of the different modelling cases.

SKB classified failure scenarios into the following categories: likely (our terminology), less probable, and residual. Likely (or probable) and less probable scenarios constitute SKB's main scenarios (scenarios that SKB considers to be risk significant), and these scenarios are included in the risk summation. No numerical probability threshold is defined for categorizing a scenario as residual. Instead, SKB classified a scenario as "residual" when SKB considered it not physically reasonable enough to occur (TR-01-11, Vol. III, pg. 568). SKB categorized scenarios related to canister failure by corrosion (due to high-flow-rate buffer erosion) and shear load (due to mechanical loads originated by seismic events) as main scenarios, and canister failure due to isostatic-load (due to glacial loading) and canister with existing pinholes at the emplacement time as residual scenarios. SKB used variants of both main and residual scenarios in what-if analyses to assess risk significance and sensitivity and to illustrate barrier functions. The variants included a number of hypothetical calculation cases in which different barriers are assumed to either gradually or suddenly degrade, as well as partially or completely lost.

2.1. General Description of SKB's Model for Release Calculations

SKB's model is briefly described. Fig. 1 shows a schematic of the SKB's near-field system and Fig. 2 shows a schematic of the various near-field components modelled. SKB's release model includes: (i) a source term representing SNF degradation, (ii) uniform mixing of dissolved radionuclides in a water volume inside the canister, (iii) radionuclide release through an opening on the canister which may grow with time, (iv) rock spalling in the deposition hole which reduces radionuclide transport resistance, (v) groundwater flow through a crown region in the deposition tunnel, (vi) radionuclide diffusion through the buffer material, (vii) diffusion and advective dispersion of radionuclides through the backfill material in the tunnels, and (viii) advective-dispersive transport of radionuclides in the geosphere.

SKB used COMP23 (Cliffe and Kelly, 2006, Kelly and Cliffe, 2006), implemented in Matlab and Simulink, as the near-field water-phase radionuclide transport model. COMP23 models radionuclide release and transport from the canister through the buffer and the deposition tunnel backfill. COMP23 accounts for radioactive decay, corrosion of contaminated structural components (modelled as a constant metal corrosion rate causing radionuclide release), SNF dissolution, dissolution of gap inventory (modelled as an instantaneous release), precipitation of

radionuclide-bearing solid phases (modelled through solubility limits), diffusion and sorption in the buffer material, and advective dispersion and sorption in the backfill of the deposition tunnel. The output of COMP23 is the rate of radionuclide release away from the near field (NF) into intercepting groundwater flow paths. To gain calculation speed, COMP23 uses analytical solutions that account for the limited size of outlets (thus offering resistance to radionuclide transport) instead of very fine discretisation around holes in the canister and around the entrance to fractures connected to groundwater flow paths.

SKB considered three fractured-rock release pathways in groundwater—labelled as Q1, Q2, Q3—through which radionuclides discharge from near-field into far-field pathways eventually releasing into the biosphere. The Q1 pathway is a fracture intersecting the deposition hole near the vertical position of the canister lid. This is the closest outlet to radionuclide releases from the canister. Thermally-induced rock spalling on the walls of deposition holes is assumed to decrease resistance to radionuclides transported through the buffer and through the rock, and discharging into the Q1 pathway. The Q2 release pathway represents the excavation damage zone (EDZ) in the floor of the backfilled tunnel. The Q3 pathway represents fractures intersecting the tunnel at a distance from the deposition hole (the farthest pathway from the canister). SKB omitted Q2 and Q3 pathways for if advective transport conditions existed between the failed canister and the Q1 pathway because of buffer erosion.

SKB's detailed hydrological modelling of fracture networks and hydrologic boundary conditions provides flow rates in the tunnel, and the distance to the nearest Q3 pathways. Transport by advection/diffusion in the tunnel is included in the near-field simulations and the computational domain is extended in the downstream direction to include the Q3 fracture. SKB estimates the Darcy flow velocity at the deposition holes and tunnels in these modelling studies.

A key aspect of the detailed hydrogeological modelling is the number of fractures intersecting deposition holes, which determines how many holes would contribute to radionuclide releases. Using the discrete fracture network (DFN) model (Data Report, Section 6.6), SKB computed flow fields for three classes of fracture correlations: semi-correlated, correlated, and uncorrelated. The correlation term refers to relationships between fracture transmissivity and fracture size. The semi-correlated class is used as the default case, and the other correlations are used for what-if cases.

SKB assumed the SNF to degrade at a constant rate. The degradation rate was varied (i.e., completely disintegrated in 100 years) to perform barrier function analysis with simultaneous loss of other barriers.

SKB used the FARF31 (Norman and Kjellbert, 1990; Elert et al., 2004) and MARFA (Painter and Mancillas, 2009) codes for far-field transport calculations. The two codes solve radionuclide transport along one-dimensional flow paths and handle advection, dispersion, matrix diffusion with equilibrium linear sorption to the rock, and radioactive decay as a part of the transport of radionuclides in the water phase. In SR-Site, groundwater flow is modelled through a DFN where individual fractures are represented explicitly. The outputs of the DFN-based flow models are groundwater travel times through one-dimensional flow paths. These flow paths and the groundwater travel times are provided as input to radionuclide transport computations in MARFA.

The main and residual canister failure conceptualizations/scenarios are described as follows and summarized in Table 1. SKB has presented results from both deterministic and probabilistic calculations.

2.2. Canister Failure Cases

2.2.1. Canister Failure by Corrosion

In the scenario for canister failure by corrosion, SKB considered that canisters fail by corrosion, after the buffer material is eroded away by fast water flow conditions in a limited number of deposition holes, predetermined by detailed hydrologic modelling. Corrosion would be caused by chemical agents, such as hydrogen sulphide, carried in groundwater. After failure by corrosion, the canister is bypassed (i.e., it offers no resistance to release) in the radionuclide release and transport computations. Similarly, SKB did not take any resistance credit by any remaining or degraded buffer material; however, SKB estimated it would take significant time (> 100,000 years) for buffer erosion and posterior canister corrosion to occur. Because of the relatively high flow rate in the fracture that intersects the deposition hole containing the failed canister, SKB assumed radionuclides to be transported solely in the Q1 release pathway (the Q2 and Q3 pathways are ignored in this scenario). SKB considered six variants of the corrosion failure scenario, one of which was defined as the central case. In this case, the canister fills up with water rapidly after failure; and the buffer is assumed to offer no transport resistance (because the buffer was eroded). With regards to the source term, SKB accounted for an instant release fraction (IRF), a corrosion release fraction (CRF) released over a relatively short period of time, and SNF degradation and dissolution at a fixed rate. SKB estimated a fractional release rate between 10^{-8} and 10^{-6} 1/yr. Radionuclides are assumed to be released congruently with the SNF matrix (predominantly uranium oxide). SKB accounted for solubility limits in the water inside the canister to control the release of radionuclides; however, in the central corrosion case solubility limits were ignored except for U and Th isotopes. SKB set the solubility limit for U and Th as zero, to retain all U and Th in the NF. Because of high flow rates that would be required for buffer erosion, SKB assumes rock retention in the far field (FF) would be smaller than expected. For the probabilistic case, the SKB model restricts multiple canister failures affecting the same biosphere object simultaneously, on the basis that less than one canister is expected to fail, and the failure time could spread over thousands of years. SKB noted that the computed flow rates at deposition holes were multiplied by a factor of 2, and that the hydraulic and transport properties were selected from the extreme tails of the distributed values output from the complex hydrogeological model, in the central corrosion case computations (SKB, 2011; TR-11-01, pg. 655).

For both deterministic and probabilistic calculations, SKB computes the contributions from the IRF to the mean dose separately from the non-IRF inventories. In the deterministic case, the IRF's contribution is determined by multiplying the IRF inventory at 100,000 years by the pulse landscape dose factor (LDF) values. In the probabilistic case, SKB first determines the probability of canister failure for each 100,000 year interval of the canister-failure-time distribution. Then it determines the total dose associated with a pulse release at the start of each 100,000-year interval. Then for each time interval, it multiplies the probability of exposure with the total dose associated with the pulse release to obtain total mean dose from release of the instant release fraction. SKB states that because

the width of the dose curves in the biosphere is typically 1,000 years, the exposure probability (due to a pulse release) at a given point in time during the 100,000 year interval is 10^{-2} and the likelihood of overlaps between pulses is very small due to the low probabilities. However, SKB includes the IRF pulse of Tc-99 in the far-field transport model calculations (hence shown in its far-field figures) since sorption in the geosphere is considerable for Tc-99.

2.2.2. Canister Failure by Shear Load

SKB considers that seismic events could cause fractures intersecting deposition holes to displace and possibly cause failure of the canister by shear load. SKB proposed a “respect distance” concept to avoid fractures of a critical size that could result in a significant displacement after a seismic event and cause canister failure. Thus, in this scenario, the number of canisters that could fail is determined by undetected fractures exceeding a critical size intercepting deposition holes, or because of errors in locating and avoiding critical fractures during repository construction. SKB modelled this scenario by (i) assuming failure of the canister at an arbitrary time between 1,000 and 1,000,000 years, (ii) assuming that the buffer material continues to function as a diffusion barrier against radionuclide transport, and (iii) not taking any credit for the presence of the canister or radionuclide retention in the geosphere. SKB assumed high fracture flow of $1 \text{ m}^3/\text{yr}$ (Q1 pathway). The Q2 and Q3 pathways were not considered for release calculations.

SKB has generally not included the IRF contributions in the shear load canister failure cases except in a few variant cases. For the distributed canister-failure-time case (i.e., 1,000 to one million years), SKB has not included IRF except for Tc-99. SKB has carried out a more detailed calculation for the initial 10,000 years period for the early canister failure case in which the IRF contributions are included.

2.2.3. Canister Failure by Isostatic Load

Isostatic-load canister failure scenario is a residual scenario for which SKB assumed that (i) the canister (both the cast iron insert and the copper shell) have failed and any protection from the canister is disregarded, (ii) the buffer surrounding the canister remains intact, and (iii) the geosphere retention properties remain. SKB hypothesized that the isostatic-load failure of the canister could cause insert buckling slightly inwards and the copper shell opening up slightly near the canister lid.

SKB calculated two canister failure cases: (i) one canister failing at 10,000 years and (ii) one canister failing at 100,000 years. SKB represented the hydrology by the semi-correlated hydrogeological DFN model and calculated flow rates for Q1, Q2, and Q3 pathways. It assumed thermally-induced spalling to occur in the wall of the deposition borehole. For dose estimation, SKB also calculated the consequence of simultaneous failure of more than one canister by scaling results from one-canister simulations, recognizing that the glacial load and locally-deficient material properties (e.g., higher than intended buffer density) could apply to more than one canister. For few simultaneous canister failures, SKB used one biosphere block, and for large simultaneous failures SKB used a spatial distribution of landscape objects, which lowers the dose (compared to cases considering only one biosphere object). SKB's treatment of IRF in the isostatic load case is not clearly stated, but SKB's

analogy of the pinhole canister failure at longer times gives the indication that IRF has been considered in this case the same way it is treated in the pinhole failure case.

2.2.4. Canister Failure by Growing Pinhole

SKB's pinhole failure scenario encompasses a hypothetical initial defect in the form of a penetrating pinhole in the copper shell, which gradually grows into a larger defect. Based on the initial state of the canisters (i.e., known initial defects), SKB believes there will be no penetrating pinhole defects in the copper shell. It assumes an initial defect to exist in the form of a pinhole in the canister wall. The pinhole offers resistance to fluid flow and radionuclide transport, because of its small size, but then it grows into a larger hole of enough dimension to no longer offer radionuclide release resistance. It considered only one canister with an initial, penetrating defect, and that water would take 1,000 years to enter and fill the canister to establish a release pathway. SKB accounted for all three release pathways (Q1, Q2, and Q3) from the NF to the FF. For the base case calculation, it assumed deposition holes to experience spalling, and that the nominal transmissivity of the EDZ was 10^{-8} m²/s. SKB analysed the effects of different EDZ transmissivities by considering probabilistic variant cases with no EDZ, and EDZ transmissivities of 10^{-6} m²/s and 10^{-7} m²/s. It considered also a flow model variant in which the tunnel backfill was compacted with a resulting gap at the tunnel crown. In this region, water was assumed to flow freely. SKB has included the IRF contributions directly in the mean dose calculation.

Table 1: Summary of scenario cases

Pinhole Case	Corrosion	Shear Load	Isostatic
-Postulated failure <ul style="list-style-type: none"> One canister with pinhole failure Release after 1,000 years of canister emplacement Pinholes instantaneously grow to large dimension after 10,000 years after emplacement -IRF included in the main calculation	-Very few canisters fail from corrosion <ul style="list-style-type: none"> high flows cause buffer erosion corrosion due to chemicals in groundwater -Iron inserts assumed to instantaneously corrode after failure by corrosion of the copper canister <ul style="list-style-type: none"> Sensitivity cases: six variant cases on the extent of corrosion failure. -Separate calculation for IRF	-Low probability (earthquake-induced) <ul style="list-style-type: none"> -Three postulated calculation cases: <ul style="list-style-type: none"> 1 canister failure at 100,000 years Distributed failure (1,000-1,000,000 years–uses pessimistic landscape dose factors) Early failure (0-10,000 years) -IRF included for the early failure case. For the distributed canister failure only Tc-99 is included. <ul style="list-style-type: none"> -Normal metal corrosion rate for CRF release -Sensitivity case: <ul style="list-style-type: none"> Shear load and buffer advection 	-Four postulated failures: <ul style="list-style-type: none"> 1 canister at 10,000 years 1 canister at 100,000 years >1 (distributed-release LDF) All canisters failed -Instant canister failure (no Cu shell, no Fe inserts failure time)
-Release resistance from canisters assumed to suddenly disappear at 10,000 years	-No release resistance from canister -Immediate radionuclide release after canister failure	-No release resistance from canister	-No release resistance from canister
-Intact buffer (i.e., buffer is a diffusive resistance barrier)	-Bypassed buffer; (i.e., radionuclides carried by flow through the canister)	-Decreased buffer thickness from 35 to 25 cm {Sensitivity cases: no buffer (i.e., flow through the canister)}	-Intact buffer
-Solubility in the in-water water	-Zero solubility limit in the in-canister water for U and Th. - Unlimited solubility for other radionuclides	-Solubility limit in the in-canister water	-Solubility limit in the in-canister water
-Q1, Q2, and Q3 pathways modelled	-Only Q1 pathway modelled	-Only Q1 pathway modelled	-Q1, Q2, and Q3 pathways modelled
-Spalling included (i.e., decreased transport resistance for Q1)	- High flow around canisters, approximately 1 m ³ /yr	- High fracture flow, approximately 1 m ³ /yr	-Spalling included (i.e., decreased transport resistance for Q1)
-EDZ transmissivity included (affects Q2 flow); 3 EDZ transmissivity alternatives	No Q2, hence EDZ transmissivity not applicable	No Q2, hence EDZ transmissivity not applicable	-EDZ transmissivity included (affects Q2 flow)
-Active tunnel swelling pressure (i.e., no crown flow in Q3 pathway in the basecase)	N/A	N/A	-Active tunnel swelling pressure (i.e., no crown flow in Q3 pathway in the basecase)
-Basecase geosphere (i.e., radionuclide retention in geosphere)	-Basecase geosphere, but low rock retention (because of high flow rates in fractures)	-No credit taken for geosphere	-Basecase geosphere (i.e., radionuclide retention in geosphere)
-Semi-correlated far field DFN	-Semi-correlated far field DFN		-Semi-correlated DFN
Global:			
-Instant breaching of cladding after canister failure			
-Normal SNF dissolution rate (fractional release rate between 10 ⁻⁸ and 10 ⁻⁶ 1/yr)			
- IRF–instantaneous release			
-CRF–release 100-10,000 years			
-Temperate climate landscape dose factor			

2.3. SKB's What-If Analysis Cases

SKB does not define criteria needed to select “what-if” analysis cases. Sensitivity analysis cases including variants of both main and residual scenarios constitute the

what-if cases. SKB used variants of the growing pinhole residual scenario in which the barrier functions were assumed to be completely lost to perform barrier function analysis.

The corrosion scenario included calculation cases constructed from a combination of hydrologic DFN alternatives, advection or no-advection conditions, transport assumptions (e.g., colloidal transport), and climatic conditions [see Fig. 4 of SKB (2010) and Fig. 13-31 of SKB (2011)]. The low-probability shear load scenario included a what-if case formed with a combination of shear load and buffer advection. SKB also conducted a variety of sensitivity studies around the “reference” case for the growing pinhole scenario: (i) advective transport in tunnels and deposition holes, (ii) sorption in tunnels and deposition holes, (iii) crown space formed by compaction of backfill in repository tunnels, (iv) varying fracture transmissivity in EDZ, and (v) assuming one or multiple transport pathways per deposition hole. For the barrier-function-loss what-if analyses, SKB considered 5 cases of assumed complete loss of different barriers as shown in Table 2.

SKB combined a loss of the radionuclide retention capability in the rock of the geosphere with each of the above five cases, yielding 10 release scenarios. In all cases it assumed that the backfill is installed and perform as expected. Also, aspects of the radionuclide transport in rock, other than those related to retention (e.g., the near-field groundwater flow, which is generally low and with only about one sixth of the deposition holes connected to water conducting fractures, as well as the stable and favourable groundwater composition in the near-field) are assumed to be described as in base case conditions. Solubility limits are imposed on concentrations of radionuclides in the canister void volume when the buffer is in place. The same approach was used in the analyses of the corrosion and shear load scenarios (TR-01-11, pg. 37).

Table 2: SKB’s what-if analysis cases—assumed complete loss of different barriers

Case	Description
A	<ul style="list-style-type: none"> •Initial absence of buffer material •Advective conditions in the deposition hole •Involves all deposition holes
B	<ul style="list-style-type: none"> •Initial pinhole in the copper shell •Involves all canisters
C	<ul style="list-style-type: none"> •Initial large opening in the copper shell and cast iron insert •Involves all canisters
D	<ul style="list-style-type: none"> •Initial absence of buffer material •Initial large opening in the copper shell and in the cast iron insert •Case A + Case C
E	<ul style="list-style-type: none"> •Initial large opening in the copper shell and in the cast iron insert •Complete fuel dissolution in only 100 years •Complete metal corrosion in only 100 years •Case C + Fast dissolution (100 years) + Fast corrosion of metal parts (100 years)

2.4. Motivation for Consultant’s assessment

The SSM staff completed an initial review phase of SR-Site documentation. SSM concluded from the initial phase of review that SKB’s reporting is sufficiently comprehensive and of sufficient quality to justify a continuation of SSM’s review to the main review phase. During the main review phase, SSM developed technical review assignments considering one or several specific issues or areas that SSM deemed to require detailed assessment. This report documents one such detailed assessment.

The objective of the work in this Technical Note is to analyse the reproducibility of SKB's computations to evaluate the transparency of the information SKB supplied and any shortcomings in SKB's analyses. Our independent analysis using models different from SKB's are intended to probe SKB's modelling approach and parameters to understand relevant input-output relationships and identify elements controlling repository performance, beyond what can be inferred from SKB reports. Another motivation of the work is to explore reasons for any significant difference between the results of SKB and our what-if analyses. A final motivation of the work is to develop a simplified model to enable to probe what-if cases that SKB may not have considered. For example, the model has already been used to evaluate the relevance of colloidal transport in another Technical Note (Pensado et al., 2014). The model was also used to examine the effect of including Rn-222 in performance assessment computations, as well as degassing of the SNF (Pensado et al., 2013).

We addressed the technical review assignment by carrying out the following tasks: (i) developing a simple model to test SKB's demonstration of the retarding capacity of the buffer, backfill, and geosphere, suitable for exploring uncertainties and sensitivities related to these repository subsystems, (ii) approximating SKB results for a few example cases, (iii) exercising a what-if calculation case different from SKB's, and (iv) identifying any potential weaknesses in the safety case based on the limited calculations and verifications. The model was exercised in deterministic and probabilistic mode.

2.4.1. General Description of the CNWRA Model

Based on our understanding of SKB's model conceptualization along with the initial and boundary conditions as described in the Radionuclide Transport Report, we developed an approximated model. The model described in Pensado and Mohanty (2012), was originally designed to approximate the corrosion and shear load canister failure scenarios. It was further modified to include capabilities for analysing isostatic load and growing pinhole canister failure scenarios. The modified model includes the main aspects described in Sections 2.1 and 2.2 of this technical note.

We considered 20 radionuclides (C-14, Cs-135, I-129, Nb-94, Ni-59, Np-237, Pb-210, Pu-239, Pu-240, Pu-242, Ra-226, Rn-222, Se-79, Tc-99, Th-230, U-233, U-234, U-235, U-236, U-238), and four decay chains (Np-237 → U-233, Pu-239 → U-235, Pu-240 → U-236, Pu-242 → U-238 → U-234 → Th-230 → Ra-226 → Rn-222 → Pb-210). SKB considered 37 radionuclides; however, Rn-222 was not explicitly modelled by SKB. The approach to estimate a LDF for Rn-222 is detailed elsewhere (Pensado and Mohanty, 2012; Pensado, et al., 2013). Initial inventories and half-lives were taken from the Data Report. Consistent with the SKB description, we considered IRF of the inventory (C-14, Cs-135, I-129, Se-79, Tc-99, Ni-59, and Nb-94) that would be immediately released into the in-canister space immediately after canister failure, and a CRF of the radionuclide inventory (C-14, Se-79, Tc-99, U-233, Ni-59, and Nb-94) present in the cladding and metallic structures that would release into the in-canister water in congruent with corrosion of these structures. Consistent with the SKB approach, we sampled the time for full depletion by corrosion from a log-triangular distribution ranging from 100 to 10,000 years, with the distribution mid-point at 1,000 years.

Mass balance computations account for decay and ingrowth. The waste form is assumed to degrade at a constant rate and radionuclides are released to the in-canister water in congruent proportion to the number of atoms in the waste form.

The time for complete degradation is sampled from a log-triangular distribution ranging from 1,000,000 to 100,000,000 years, with the mid-point of the distribution at 10,000,000 years. Radionuclides are released into 1 m³ of in-canister water and are assumed to be uniformly mixed. Precipitation and dissolution back into the solution is allowed to occur depending on whether the concentration is above or below the solubility limit.

Far-field mass transport is modelled as presented in a previous technical note (Pensado and Mohanty, 2012) except that now we included all three release pathways, Q1, Q2, and Q3. The model accounts for advective-dispersive transport along one-dimensional pathways, representing transport along fractures. Matrix diffusion causes mass exchange between fractures and the rock matrix along a direction perpendicular to the flow direction. Equilibrium linear sorption operates in the rock matrix. The main parameters of interest in the current model are the canister failure time, the rock transport resistance (F), the advective travel time (t_w), and the advective flow through the deposition hole (q).

For stochastic simulations, we used the values in Table 4-3 of the Radionuclide Transport Report. For the stochastic simulations, SKB used those discrete values repeatedly in the multiple-realizations, but for our model, cumulative distribution functions (CDF) were established for parameter such as $\log(F)$, $\log(t_w)$, and q for sampling. The canister failure time was sampled from a uniform distribution constructed from data in Table 4-3 of the Radionuclide Transport Report (i.e., minimum and maximum times of 114,486 years and 978,463 years in Table 4-3). A correlation coefficient between $\log(F)$ and $\log(t_w)$ of 0.88 was also computed from Table 4-3.

As was done in Pensado and Mohanty (2012), LDF and pulse LDF for temperate conditions are used to convert radionuclide release rates in units of activity/time into release rates in units of dose per year. Temperate LDF flat pulse doses are used for a relatively short period. For longer periods, LDF values were used. The pulse LDF values were only used to compute near-field doses. Temperate LDF was used to translate FF release rates in units of Bq/yr to doses in units of Sv/yr in the deterministic computations. Consistent with SKB's approach, we disregarded IRF (and hence, pulse LDF) in our computations for the stochastic simulations (i.e., the IRF was set equal to zero, and continuous LDF values were used) in the corrosion and shear load scenarios. We only used pulse LDF values in the deterministic computations of near-field doses in the corrosion failure scenario. In the computations for the growing pihole scenario and canister failure by isostatic load scenarios, we considered the IRF contribution in both deterministic and probabilistic simulations.

2.4.2. Setting up the Model

Fig. 2 shows the schematic of various components represented in our simplified model. Blocks 1, 2, and 3, and release through the Q1 pathway were modelled in Pensado and Mohanty (2012). Q2 and Q3 pathways have been added to the current version of the model by explicit inclusion of remainder of the blocks, as well as implementation of the blocks representing the p and f plugs. These plugs are numerical corrections (needed due to the coarse discretization of the system) to account for transfer resistance due to the small canister pinhole size, and narrow fracture aperture in the host rock.

Block 6 in Fig. 2 represents the backfill above the buffer at the top of the canister in a deposition hole. Block 6 is linked to the Q2 pathway with an advective transport connection and to Block 7 (i.e., the tunnel) with a diffusive transport connection. Block 7 represents the backfill in the tunnel. Block 7 is a horizontal cylinder with 5 discrete layers stacked the vertical direction with diffusion-only vertical connections. Likewise, 7 discrete compartments are used in Block 7 along the length of the tunnel (5 of these to the downstream of the deposition hole position, one to the upstream of the deposition hole, and one above the deposition hole) with diffusive and advective transport connections. The length of the downstream compartments is a function of the distance between the deposition hole and the first fracture in the deposition tunnel, which is treated as an uncertain parameter and thus varies from realization to realization. The vertical thickness of the layers is 0.8 m except that the top 0.1 m of the top layer represents the crown void space block, and is treated as a separate layer. The entire radionuclide mass crossing a vertical plane, perpendicular to the tunnel axis, at the end of the tunnel is assumed to discharge into the Q3 fracture. The flow for the advective connection between the “end” of the tunnel element (i.e., the element connected to the Q3 pathway) and Q3 is assumed to equal the Q3 fracture flow plus the total flow through the tunnel plus the flow through the void crown space, if applicable.

For probabilistic analyses, the distance between the deposition hole and the nearest fracture in the deposition tunnel (see Fig. 1 and Block 7 in Fig. 2) mentioned above was estimated from data from Joyce et al. (2010) (see TR-10-50; Section G.7, pg. 316). The following distances to fractures were considered along with their frequency of occurrence: <2.5 m (10%), <6.82 m (72%), <10.26 m (88%), <44.82 m (99%), and <103.8 m (99.8%). This information was approximated by a log-normal distribution with a median equal to 5.1 m, and a standard deviation equal to 8.5 m. The mean of this log-normal distribution is 7.6 m. For deterministic cases, we used the median value of 5.1 m.

For deterministic calculations, we used median values of transport parameters such as Darcy velocity and equivalent flow rates reported by SKB in Table 3-5 of TR-10-50 (U01, Qeq1, Qeq2, and Qeq3) and water travel time (t_w) and resistance factors (F) for the three release pathways (Q1, Q2, and Q3). For probabilistic calculations, we estimated distribution functions for these parameters based on information in R-09-20 (Joyce et al., 2010). This report provides normalized CDF plots of Qeq values and tunnel flows, U_r , derived from SKB hydrogeological model for the particles, released at a certain time, successfully reaching the top boundary in the model. We verified that the CDFs in the report R-09-20 are approximately log-normal. Accordingly, for probabilistic simulations, we adopted lognormal distributions for Qeq1, Qeq2, Qeq3, U_r , t_w and F , with median values as in Table 3-5 of TR-10-50, and geometric standard deviations as in Table 3. The geometric standard deviations were estimated from plots in the report R-09-20.

2.4.3. Confirmation of What-If Calculations

Our confirmatory calculations primarily focused on the residual scenario pinhole canister failure case because it is a case that has all engineered and geosphere components in place, thus it is convenient for numerically experimenting the what-if cases for testing the retarding capacity of the buffer and the geosphere and for exploring uncertainties related to these components of the repository. Furthermore, the pinhole case allows understanding the consequences of a large defect, which

Table 3: Parameters of lognormal distributions in probabilistic simulations

Parameter	Lognormal distribution parameters		Source
F1	Median	4×10^6 yr/m	Median from Table 3-6 in TR-10-50 (isostatic load, pinhole base case and no spalling). Geometric SDev estimated from TR-10-52, Fig. 6-67.
	Geometric SDev	5.6	
	Mean	1.76×10^7 yr/m	
	SDev	7.57×10^7 yr/m	
F2	Median	2.3×10^6 yr/m	Median from Table 3-6 in TR-10-50 (isostatic load, pinhole base case and no spalling). Geometric SDev estimated from TR-10-52, Fig. 6-67.
	Geometric SDev	5.6	
	Mean	1.01×10^7 yr/m	
	SDev	4.35×10^7 yr/m	
F3	Median	1.9×10^6 yr/m	Median from Table 3-6 in TR-10-50 (isostatic load, pinhole base case and no spalling). Geometric SDev estimated from TR-10-52, Fig. 6-67.
	Geometric SDev	5.6	
	Mean	8.38×10^6 yr/m	
	SDev	3.6×10^7 yr/m	
t_{w1}	Median	180 years	Median from Table 3-6 in TR-10-50 (isostatic load, pinhole base case and no spalling). Geometric SDev estimated from TR-10-52, Fig. 6-67.
	Geometric SDev	2.84	
	Mean	310.2 years	
	SDev	435.3 years	
t_{w2}	Median	160 years	Median from Table 3-6 in TR-10-50 (isostatic load, pinhole base case and no spalling). Geometric SDev estimated from TR-10-52, Fig. 6-67.
	Geometric SDev	2.84	
	Mean	275.7 years	
	SDev	386.9 years	
t_{w3}	Median	150 years	Median from Table 3-6 in TR-10-50 (isostatic load, pinhole base case and no spalling). Geometric SDev estimated from TR-10-52, Fig. 6-67.
	Geometric SDev	2.84	
	Mean	258.5 years	
	SDev	362.8 years	
Qeq1	Median	4.2×10^{-6} m ³ /yr	Median from Table 3-5 in TR-10-50 (isostatic load, pinhole base case and no spalling). Geometric SDev estimated from R-09-20 Fig. E-5.
	Geometric SDev	4.67	
	Mean	1.38×10^{-5} m ³ /yr	
	SDev	4.3×10^{-5} m ³ /yr	
Qeq3	Median	1.2×10^{-4} m ³ /yr	Median from Table 3-5 in TR-10-50 (isostatic load, pinhole base case and no spalling). Geometric SDev estimated from R-09-20 Fig. E-5.
	Geometric SDev	2.87	
	Mean	2.1×10^{-4} m ³ /yr	
	SDev	2.98×10^{-4} m ³ /yr	
Tunnel velocity (Ur)	Median	1.17×10^{-5} m/yr	Median from Table 3-5 in TR-10-50 (isostatic load, pinhole base case and no spalling) computed as TRAPP_3*LR_TUN_3/TR_TUN_3. Geometric SDev estimated from R-09-20 Fig. E-4 (based on UR3).
	Geometric SDev	5.3	
	Mean	4.75×10^{-5} m/yr	
	SDev	1.86×10^{-4} m/yr	
Qeq2	Computed as Ur*Qeq2(median)/Ur(median)		Median from Table 3-5 in TR-10-50. Qeq2 is assumed perfectly correlated to Ur.
	Median	9.3×10^{-5} m/yr	

resembles the case of a failure caused by general corrosion of the canister when the buffer is still intact. However, SKB attributes the likelihood of this latter failure mode negligible in the analysis of the corrosion scenario (TR-01-11, Section 12.6).

However, before conducting calculation involving the pinhole scenario, we tested the reproducibility of the calculations involving the main scenarios (i.e., corrosion and shear load failure) reported in Pensado and Mohanty (2012). We briefly mention those results here as a comparison with the SKB results without presenting the corresponding figures. Table 4 provides a summary of all peak dose equivalent release (DERs) from deterministic and probabilistic (mean value) calculations.

Our corrosion failure scenario's deterministic calculation showed a peak NF DER of 35.8 $\mu\text{Sv}/\text{yr}$ at 115,200 yr and an FF peak DER of 5.4 $\mu\text{Sv}/\text{yr}$ at 615,000 yr. SKB's calculation showed a peak NF DER of 22 $\mu\text{Sv}/\text{yr}$ at 114,485 and an FF peak DER of 3.2 $\mu\text{Sv}/\text{yr}$ at ~1,000,000 years. The trends in the radionuclide releases as a function of time were very similar (almost identical). Clearly, SKB's results were reproducible within a factor of 2. Our probabilistic calculation of the corrosion failure scenario showed a peak NF DER of 5.21 $\mu\text{Sv}/\text{yr}$ at 1,000,000 years with a standard deviation of 15.03 $\mu\text{Sv}/\text{yr}$ and a peak FF DER of 0.19 $\mu\text{Sv}/\text{yr}$ at 1,000,000 years with a standard deviation of 0.27 $\mu\text{Sv}/\text{yr}$. This is in contrast with SKB's peak NF DER of 0.59 $\mu\text{Sv}/\text{yr}$ at 1,000,000 years and peak FF DER of 0.18 $\mu\text{Sv}/\text{yr}$ at 1,000,000 years. Therefore, the FF results compare very well. The difference in the NF results is due to an excess release of Pb-210, which appears to be a numerical artefact in our simple model.

Our shear load failure scenario deterministic calculation showed peak NF and FF DER of 5.64 $\mu\text{Sv}/\text{yr}$ at 101,400 yr. SKB's deterministic calculation showed a peak DER of 5.6 $\mu\text{Sv}/\text{yr}$ at 100,000 yr, which is almost identical to our results. Our probabilistic calculation of the shear load failure scenario showed a peak NF of FFDER of 6.22 $\mu\text{Sv}/\text{yr}$ at 1,000,000 years. This value is comparable to SKB's peak DER of 4.2 $\mu\text{Sv}/\text{yr}$ at ~7,000 years.

The following are the baseline growing pinhole failure case, isostatic load failure case, and several what-if cases analysed, some of which are an attempt to test the reproducibility of SKB's results (Cases 1, 2, 3, and 4) and others (Cases 5 and 6) are the new cases, which, as far as we can tell, are not analysed by SKB.

Case -1- Growing Pinhole

Deterministic

SKB's Growing Pinhole Case deterministic calculations [Fig. 3(a)-bottom] show a peak NF DER of 9.5 $\mu\text{Sv}/\text{yr}$ at 10,000 yr with C-14 and I-129 being the dominant contributors at and before ~10,000 yr. The C-14 contribution drops sharply in the first 55,000 years. I-129 becomes the dominant radionuclides after ~10,000 years and remains so until 1,000,000 years, the end of the simulation period. The Se-79 DER approaches that of I-129 after ~150,000 years.

Our Growing Pinhole Case deterministic calculations [Fig. 3(a)-top] show a peak NF DER of 8.73 $\mu\text{Sv}/\text{yr}$ (5.4 $\mu\text{Sv}/\text{yr}$ with no IRF) at 10,100 years with C-14 and I-129 being the dominant contributors at and before ~10,000 years. The C-14 contribution drops sharply in the first 60,000 years. I-129 becomes the dominant radionuclides after ~10,000 years and the Se-79 DER approaches that of I-129 contribution beyond 200,000 years. The shape of the DER curves for other radionuclides, especially Se-79, Ni-59, Nb-94, and Ra-226, appear identical to those of SKB's.

In SKB's deterministic NF calculation [Fig. 3(b)-bottom] the NF release is dominated by the Q1 pathway during the entire simulation period. Q2 pathway release dominates the Q3 pathway release before 20,000 years where Q3 pathway dominates Q2 pathway for the rest of the simulation period. Q2 and Q3 pathway release peaks show the shape consistent with the longer distance the radionuclides must travel for release from the NF. Our deterministic NF calculations [Fig. 3(b)-top] show very similar results, as shown in those of SKB's.

Table 4: Peak DERs from deterministic and probabilistic calculations for various modelling cases

Calculation case	SKB analysis–deterministic		SKB analysis–probabilistic		Our analysis–deterministic		Our analysis–probabilistic	
	NF	FF	NF	FF	NF	FF	NF	FF
Corrosion	22	3.2	.59	.18	35.8	5.4	5.21	0.19
Shear load	5.6	5.6	4.2	4.2	5.64	5.64	6.22	6.22
Pinhole	9.5	1.6	3.7	.65	8.73	2.63	13.14	3.4
Isostatic (10,000 year failure)	7	1.6	2.5	0.63	6.06	1.48	9.04	2.4
Isostatic (100,000 year failure)	4.5	1.5	1.5	.39	3.11	1.09	4.5	1.46
Growing Pinhole + Crown Flow (Q3 Fracture at 118 m)	16	10	9.5	2.7	9.75	8.31	13.3	7.69
Corrosion with initial advection	154	3.6	1	.27	39.4	6.1	.779	.27
Growing Pinhole + Crown Flow (Q3 Fracture at 5.1 m)	-	-	-	-	35.72	26.19	31.65	18.87
Corrosion failure + Fast SNF degradation	22	3.2	.59	.18	36.17	5.47	.13	.12

SKB's FF release calculations [Fig. 3(c)-bottom] show a peak DER of 1.6 $\mu\text{Sv}/\text{yr}$. I-129, C-14, and Se-79 are the only radionuclides that appear prominently. I-129 is the dominant radionuclide during most of the simulation period. C-14 contribution drops sharply in the first ~60,000 years. I-129 contribution to peak is little less than an order of magnitude higher than C-14. The pathway release rates are almost identical to the NF release trends [Fig. 3(d)-bottom].

Ours deterministic calculations [Fig. 3(c)-top] show a mean FF peak DER of 2.63 $\mu\text{Sv}/\text{yr}$ (0.82 $\mu\text{Sv}/\text{yr}$ with no IRF) at 12,350 years. C-14 is the marginally dominant contributor before ~10,000 years and I-129 is the dominant radionuclide after 10,000 years. Similar to SKB's results, C-14 contribution drops sharply in the first ~65,000 years. I-129 contribution to peak is about an order of magnitude higher than C-14. Our calculations show the FF pathway release trend [Fig. 3(d)-top] identical to that of our NF calculation [Fig. 3(b)-top] except the expected time lag.

Probabilistic

SKB probabilistic results for the pinhole case [Fig. 3(e) to 3(h)-bottom] were very similar to that of the deterministic case [Fig. 3(a) to 3(d), bottom] described above, in terms of the list of radionuclides showing prominently as DER contributors, the dominance of specific radionuclides in NF and FF releases, the dominance of release pathways in NF and FF releases. SKB's probabilistic results show a peak NF DER of 3.7 and peak FF DER of 0.65 $\mu\text{Sv}/\text{yr}$ [Figs. 3(e) and 3(g) –bottom]. SKB's calculations show that NF Q1 release dominates until about 15,000 years, followed by Q2 and Q3 [Fig. 3(f)-bottom]. Beyond 15,000 years, Q3 pathway release dominates, followed by Q2 and Q1. The total DER at 1,000,000 years was 0.3 $\mu\text{Sv}/\text{yr}$ for NF and .16 for FF [Figs. 3(f) and 3(h)–bottom].

Our probabilistic calculations show a peak NF DER of 13.14 $\mu\text{Sv}/\text{yr}$ at 10,100 years [Fig. 3(e)-top] with a standard deviation at the peak of 12.1 $\mu\text{Sv}/\text{yr}$. The corresponding DER and standard deviations for the no-IRF case are 8.57 and 8.2 $\mu\text{Sv}/\text{yr}$.

Our probabilistic calculations show a peak FF DER of 3.4 $\mu\text{Sv}/\text{yr}$ [Fig. 3(g)-top] with a standard deviation at the peak of 4.04 $\mu\text{Sv}/\text{yr}$. The corresponding DER and standard deviations for the no-IRF case are 1.604 $\mu\text{Sv}/\text{yr}$ and 2.17 $\mu\text{Sv}/\text{yr}$, respectively. The trends in radionuclide-specific curves were identical that of the deterministic case, and that of SKB's.

Our probabilistic FF release results are somewhat higher than SKB's but the trends are almost identical. Our calculations show that Q1 release dominates over the entire simulation period. Q1 release > Q2 release > Q3 release at less than 20,000 years. Beyond this period, Q3 release > Q1 release. Our calculations showed an all-pathway peak DER of 0.43 $\mu\text{Sv}/\text{yr}$ for NF and 0.22 for FF, respectively [Fig. 3(h)-top].

Overall, our radionuclide-release trends, radionuclides showing up as dominant, the pathway release rates are similar and in most cases identical to that of SKB's, for both NF and FF, before and after 10,000 years, thus SKB results are reproducible for the Growing Pinhole Case.

Case 2- Isostatic Failure:

Canister Failure at 10,000 Years

Deterministic

SKB's Isostatic Case deterministic calculations for 10,000-years canister failure time [Fig. 4(a)-bottom] show a peak NF DER of 7 $\mu\text{Sv}/\text{yr}$ at 11,000 years with I-129 and C-14 being the dominant contributors. I-129 is the dominant radionuclides for the entire simulation period, with Se-79 contribution approaching it after ~250,000 years.

Our Isostatic Case deterministic calculations [Fig. 4(a)-top] show a peak NF DER of 6.06 $\mu\text{Sv}/\text{yr}$ at 11,000 years with radionuclide contribution trend being identical to that of SKB's.

SKB's FF release calculations [Fig. 3(b)-bottom] show a peak DER of 1.6 $\mu\text{Sv}/\text{yr}$ at 15,000 years. I-129 is the major contribution, followed by C-14, and Se-79. I-129 is the dominant radionuclide during most of the simulation period. C-14 contribution drops sharply in the first ~70,000 years.

Ours deterministic calculations [Fig. 3(c)-top] show a mean peak FF DER of 1.48 $\mu\text{Sv}/\text{yr}$ at 14,150 years. The radionuclide release trends are identical to that of SKB's.

Probabilistic

SKB probabilistic results for the Isostatic case [Figs. 4(c) and 4(d)-bottom] were very similar to those of the deterministic case [Figs 4(a) to 4(d), bottom] described above, in terms of the list of radionuclides showing prominently as DER contributors, the dominance of specific radionuclides in NF and FF releases. SKB's

probabilistic results show a peak NF DER of 2.5 and peak FF DER of 0.63 $\mu\text{Sv}/\text{yr}$ at 10,000 years [Figs. 3(c)–bottom].

Our probabilistic calculations show a mean peak NF DER of 9.04 $\mu\text{Sv}/\text{yr}$ at 11,000 years [Fig. 3(c)-top] with a standard deviation at the peak of 8.2 $\mu\text{Sv}/\text{yr}$. The trend in radionuclides release is identical to that of SKB's.

Our probabilistic calculations show a mean peak FF DER of 2.4 $\mu\text{Sv}/\text{yr}$ at 12,350 years [Fig. 3(d)-top] with a standard deviation at the peak of 3.4 $\mu\text{Sv}/\text{yr}$. The trends in radionuclide-specific curves were identical that of the deterministic case, and that of SKB's.

Canister Failure at 100,000 Years

SKB's Isostatic Case deterministic calculations for 100,000-years canister failure time show a peak NF DER of 4.5 $\mu\text{Sv}/\text{yr}$ at 100,000 years.

Our Isostatic Case deterministic calculations show a peak NF DER of 3.11 $\mu\text{Sv}/\text{yr}$ at 101,400 years. SKB's deterministic FF release calculations show a peak DER of 1.5 $\mu\text{Sv}/\text{yr}$ at 100,000 years. Our deterministic calculations show a mean FF peak DER of 1.09 $\mu\text{Sv}/\text{yr}$ at 105,600 years. The radionuclide release trends are identical to that of SKB's for both NF and FF release calculations.

SKB probabilistic results for the Isostatic case were very similar to that of the deterministic case in terms of the list of radionuclides showing prominently as DER contributors, the dominance of specific radionuclides in NF and FF releases. SKB's probabilistic results show a peak NF DER of 1.5 and peak FF DER of 0.39 $\mu\text{Sv}/\text{yr}$ at 100,000 years.

Our probabilistic calculations show a mean peak NF DER of 4.5 $\mu\text{Sv}/\text{yr}$ at 101,400 years with a standard deviation at the peak of 4.17 $\mu\text{Sv}/\text{yr}$. Our probabilistic calculations show a mean peak FF DER of 1.46 $\mu\text{Sv}/\text{yr}$ at 103,500 years with a standard deviation at the peak of 2.03 $\mu\text{Sv}/\text{yr}$. The trends in radionuclide-specific curves were identical that of the deterministic case, and that of SKB's.

Overall, for the Isostatic Load case, our peak NF and FF DERs from both deterministic and probabilistic calculations are close to SKB's (within a factor of 5). Our deterministic results have a better match than the probabilistic results for both 10,000 years and 100,000-years canister failure times. Deterministic results deviate from SKB results by less than 20%. In both our and SKB's calculations I-129, Se-79, Ra-226, and Ni-59 show up as the primary contributors to the NF DER, and I-129, Se-79, and Ra-226 show up as the primary contributors to the FF DER. The trends in the DER at the radionuclide level as a function of time are almost identical in both our and SKB's case.

Case 3- Growing Pinhole + Crown Flow:

For creating this case, the flux value was adjusted for the crown space to reflect SKB's LR_TUN_3 value of 118 m and TR_TUN_3 value of 890 years, which resulted in a flux value in the crown space of ~ 0.13 m/yr (i.e., 1×118 m/890 years, where 1 reflects that the porosity of the crown is 100%). The median value of the deposition tunnel–Q3 fracture intersection was specified to be 118 m.

Deterministic

SKB's Growing Pinhole with Crown Flow Case deterministic calculations [Fig. 5(a)-bottom] show a peak NF DER of 16 $\mu\text{Sv}/\text{yr}$ at $\sim 12,000$ years with C-14 and I-129 being the dominant contributors, respectively, at and before $\sim 20,000$ years. The C-14 contribution drops sharply in the first 40,000 years. I-129 is the dominant radionuclides beyond $\sim 20,000$ years and only after nearly 250,000 years another radionuclide, which is Se-79 in this case, matches with that of I-129 contribution. The release rate at 1,000,000 years is ~ 0.26 $\mu\text{Sv}/\text{yr}$.

SKB's deterministic NF calculation [Fig. 5(b)-bottom] shows that the Q2 release pathway has the lowest release rate. Q1 release pathway dominates for about 1,000 years after release and after $\sim 20,000$ years. Q3 release dominates rest of the simulation period.

SKB's deterministic FF release calculations [Fig. 5(c)-bottom] show a peak FF DER of 10 $\mu\text{Sv}/\text{yr}$ at $\sim 13,000$ years with C-14 being the dominant contributor until about 15,000 years. I-129 is the dominant radionuclides beyond $\sim 15,000$ years. The release rate at 1,000,000 years is ~ 0.18 $\mu\text{Sv}/\text{yr}$.

SKB's calculations for the FF [Fig. 5(d)-bottom] shows an almost identical trend as the NF except that the peaks show a greater time lag, as expected, except that Q3 pathway release overtakes the Q1 pathway release somewhat earlier.

Our Growing Pinhole with Crown Flow Case deterministic calculations [Fig 5(a)-top] show a peak NF DER of 9.75 $\mu\text{Sv}/\text{yr}$ at 14,150 years with C-14 being the dominant contributor until $\sim 15,000$ years and I-129 thereafter. The C-14 contribution drops sharply in the first 40,000 years, similar to that of SKB's. After $\sim 100,000$ years Se-79 DER matches with that of I-129 contribution. The release rate at 1,000,000 years is 0.275 $\mu\text{Sv}/\text{yr}$.

In our NF calculation [Fig. 5(b)-top], the NF release is dominated by the Q1 and Q3 pathways. The first 400 years after the onset of the release and for 2,000 years after 10,000-years spike, Q1 pathway release dominates. The rest of the period is dominated by the Q3 pathway release. But unlike SKB results, Q1 pathway release in our calculation dominates the Q2 pathway release over the entire simulation period. Peaks from all three pathways occur at $\sim 10,000$ years with slight lags in Q2 and Q3 pathways, consistent with the distance from the canister.

Our Growing Pinhole with Crown Flow Case deterministic calculations [Fig. 5(c)-top] show a peak FF peak DER of 8.31 $\mu\text{Sv}/\text{yr}$ at 15,050 years with radionuclide release trend similar to that of NF, with C-14, I-129, and Se-79 being the primary contributors, which is similar to SKB's. The release rate at 1,000,000 years is 0.2 $\mu\text{Sv}/\text{yr}$.

Probabilistic

SKB's Growing Pinhole with Crown Flow Case probabilistic calculations [Fig. 5(e)-bottom] show a peak NF peak DER of 9.5 $\mu\text{Sv}/\text{yr}$ at 10,000 years with C-14 and I-129 being the dominant contributors at and before $\sim 10,000$ years (C-14 peak 5 times higher than the I-129 peak). The C-14 contribution drops sharply in the first 50,000 years. I-129 becomes the dominant radionuclides after $\sim 20,000$ years and only after nearly 250,000 years another radionuclide, which is Ra-226 in this case, matches with that of I-129 contribution.

In SKB's NF calculation [Fig. 5(f)-bottom] the NF release is dominated by the Q3 pathway during the entire simulation period, except the first 1,000 years after the onset of the release. Q1 pathway release dominates the Q2 pathway release 10,000 years. After ~15,000 years, Q2 pathway release overtakes the Q1 pathway release. Peaks from all three pathways occur at ~10,000 years with slight lags in Q2 and Q3 pathways, consistent with the travel distance from the canister.

SKB's Growing Pinhole with Crown Flow Case probabilistic calculations [Fig. 5(f)-bottom] show a peak FF DER of 2.7 $\mu\text{Sv}/\text{yr}$ at 10,000 years with C-14 and I-129 being the dominant contributors at and before ~10,000 years (C-14 peak ~5 times higher than the I-129 peak). The C-14 contribution drops sharply in the first 50,000 years. I-129 becomes the dominant radionuclides after ~15,000 years. Se-79 and Ra-226 are distant third and fourth radionuclides contributing to DER.

SKB's calculations for the FF [Fig. 5(h)-bottom] shows an almost identical trend as that of the NF calculations for pathway-specific releases except that the peaks show a greater time lag (as expected) except that Q2 pathway release overtakes the Q1 pathway release somewhat earlier.

Our Growing Pinhole with Crown Flow Case probabilistic calculations [Fig. 5(e)-top] shows a peak NF DER of 13.35 $\mu\text{Sv}/\text{yr}$ at 10,200 years with a standard deviation at the peak of 12.36 $\mu\text{Sv}/\text{yr}$. C-14 and I-129 are the dominant contributors at and before ~10,000 years (C-14 peak 6 times higher than the I-129 peak). The C-14 contribution drops sharply in the first 50,000 years similar to that of SKB's. I-129 becomes the dominant radionuclides after ~15,500 years and after ~250,000 years Ra-226 DER matches with that of I-129 contribution.

Ours Growing Pinhole with Crown Flow Case probabilistic calculations [Fig. 5(g)-top] show a mean FF peak DER of 7.69 $\mu\text{Sv}/\text{yr}$ at 12,350 years with a standard deviation at the peak of 8.05 $\mu\text{Sv}/\text{yr}$. C-14 and I-129 are the dominant contributors at and before ~10,000 years. Similar to SKB's results, C-14 contribution drops sharply in the first 55,000 years and I-129 becomes the dominant contributor after ~20,000 years with about a factor of 5 above Se-79, the next nearest contributor. Ra-226's contribution to DER is more than an order of magnitude below I-129.

In our NF calculation [Fig. 5(f)-top], the NF release is dominated by the Q1 and Q3 pathways, Q1 dominates during the first 300 years after the onset of the release and for 1,500 years after the 10,000-years spike. But unlike SKB results, Q1 pathway release in our calculation dominates the Q2 pathway release over the entire simulation period. Peaks from all three pathways occur at ~10,000 years with slight lags in Q2 and Q3 pathways, consistent with the distance from the canister.

Our calculations [Fig. 5(h)-top] show the FF pathway release trend is more or less identical to that of our NF calculation except the expected time lag.

Overall, our radionuclide-release trends are similar to that of SKB's, both NF and FF and before and after 10,000 years. Our peak NF and FF DERs are close to that of SKB's. Our DERs at 1,000,000 years matches well with SKB's. In our calculations Q1 release dominates over Q2 pathway release throughout the simulation period whereas in SKB's calculation the Q2 pathway release exceeds that of Q1 release most of the simulation period.

Case 4:

In this what-if case, the central corrosion scenario was varied by adding initial advection. In all our calculations, unlimited solubility limits were used except for U and Th, which were assumed to be very low. SKB's initial advection calculation led failure to occur as early as 44,049 years compared to the earliest failure time of 114,485 years for the corrosion scenario without initial advection. For the deterministic case, 1 canister was specified to have failed at 44,049 years whereas in the probabilistic case, the canister failure distribution was obtained by simply specifying the lower end of the failure time range to be 44,049 years.

SKB's deterministic calculation [Figs. 6(a) and (b)] showed a peak DER of 154 $\mu\text{Sv}/\text{yr}$ for NF and FF DER of 3.6 $\mu\text{Sv}/\text{yr}$ at the canister failure time of 44,049 years.

Our deterministic calculation showed a peak NF DER of 39.7 $\mu\text{Sv}/\text{yr}$ at 52,000 years and FF DER of 6.1 $\mu\text{Sv}/\text{yr}$ at 595,000 years, which compared well with SKB's. Results match within a factor of 2.

SKB's probabilistic calculation [Figs. 6(c) and (d)] showed mean peak NF and FF DERs of 1 and 0.27 $\mu\text{Sv}/\text{yr}$, respectively, both occurring at 1,000,000 years. For NF release, Ra-226, Nb-94, Pb-210, and Np-237 were dominant radionuclides whereas for FF release Ra-226, I-129, Np-237, and Se-79 were the dominant radionuclides.

Our probabilistic calculation (100 realizations) showed a peak NF DER of 0.779 at 1,000,000 years and an FF DER of 0.2722 occurring at 1,000,000 years. Ra-226, Pb-210, and Np-237 were the main NF DER contributors whereas for FF DER, Ra-226, Rn-222, Se-79, I-129, and Np-23 were the major contributors. Therefore, our calculation reproduced SKB's calculations fairly well for this case.

Case 5:

In SKB's nominal growing pinhole + crown flow scenario case, the distance between the deposition hole position in the tunnel and the fracture intersecting the tunnel in the Q3 pathway is 118 m [see Table 3-5 of TR-10-50, pg53 (SKB, 2010)]. However, in its growing pinhole scenario case, SKB uses a distance of 5.1 m for hydrogeologic calculations. It is not clear why SKB used 118 m instead of 5.1 m. This what-if case involves estimating the impact of the Q3 fracture intersecting the tunnel at 5.1 m instead of 118 m.

Deterministic

Our Growing Pinhole + Crown Flow Case deterministic calculations with the Q3 fracture intersecting the tunnel at 5.1 m show a peak NF DER of 35.715 $\mu\text{Sv}/\text{yr}$ at 11,000 years [Fig. 7(a)], with C-14 being the dominant contributor until ~15,000 years and I-129 thereafter. The C-14 contribution drops sharply in the first 40,000 years. After ~80,000 years Se-79 DER matches with that of I-129 contribution. The release rate at 1,000,000 years is ~.4 $\mu\text{Sv}/\text{yr}$.

In our NF calculation [Fig. 7(b)], the NF release is dominated by the Q3 pathway during the entire simulation period, except the first 500 years after the onset of the release. Q1 pathway release dominates the Q2 pathway release over the entire simulation period. Peaks from all three pathways occur at ~10,000 years with slight lags in Q2 and Q3 pathways, consistent with the distance from the canister.

Our Growing Pinhole with Crown Flow Case deterministic calculations [Fig. 7(c)] show a peak FF DER of 26.19 $\mu\text{Sv}/\text{yr}$ (21.46 $\mu\text{Sv}/\text{yr}$ with no IRF) at 11,900 years with radionuclide release trend similar to that of NF, except that Ra-226 release was much lower. Fig. 7(d) shows the path-specific DERs for FF release for the deterministic case. The release rate at 1,000,000 years is $\sim 0.165 \mu\text{Sv}/\text{yr}$.

Probabilistic

Our Growing Pinhole with Crown Flow Case probabilistic calculations [Fig. 7(e)-top] shows a peak NF DER of 31.65 $\mu\text{Sv}/\text{yr}$ at 10,900 years with a standard deviation at the peak of 14.65 $\mu\text{Sv}/\text{yr}$. C-14 and I-129 are the dominant contributors at and before $\sim 10,000$ years (C-14 peak 6 times higher than the I-129 peak). The C-14 contribution drops sharply in the first 50,000 years. I-129 becomes the dominant radionuclides after $\sim 15,500$ years and after $\sim 250,000$ years Ra-226 DER matches with that of I-129 contribution. At the realization level, the peak DER values range between 3.5 at 11,000 years and 72.4 at 10,600 years, with a median value of 26.9 at 11,000 years.

In our NF calculation [Fig. 7(f)-top], the NF release is dominated by the Q3 pathway during the entire simulation period, except the first 500 years after the onset of the release. Q1 pathway release in our calculation dominates the Q2 pathway release over the entire simulation period. Peaks from all three pathways occur at $\sim 10,000$ years with slight lags in Q2 and Q3 pathways, consistent with the distance from the canister.

Our probabilistic calculations [Fig. 7(g)-top] show a mean peak FF DER of 18.87 $\mu\text{Sv}/\text{yr}$ at 11,900 years with a standard deviation at the peak of 11.4 $\mu\text{Sv}/\text{yr}$. The corresponding peak-of-the-mean and standard deviations are 14.78 and 9.17 $\mu\text{Sv}/\text{yr}$ for the no-IRF case. C-14 and I-129 are the dominant contributors at and before $\sim 10,000$ years. C-14 contribution drops sharply in the first 55,000 years and I-129 becomes the dominant contributor after $\sim 20,000$ years with about an order of magnitude above Se-79, the next nearest contributor. Ra-226 DER does not catch up with the I-129 as a significant contributor. At the realization level, the peak DER values range between 2.7 at 14,600 years and 61.5 at 11,000 years, with a median value of 24.9 at 11,900 years. Fig. 7(h) shows the path-specific DERs for FF release in the probabilistic case.

Overall, our calculations show that the peak NF and FF DERs are higher than the 118-m case by a factor of 2 to 3. Moreover, in our calculations Q1 release dominates over Q2 pathway release throughout the simulation period whereas in SKB's calculation the Q2 pathway release exceeds that of Q1 release most of the simulation period. Consequently, a change to the median tunnel-Q3 fracture distance from 118 m to from 5.1 m (standard deviation being kept the same as before), does not result in a significant change in the DER.

Case 6:

In this what-if case, the central corrosion scenario was varied by accelerating the SNF degradation rate from $1 \times 10^{-7}/\text{yr}$ to $1 \times 10^{-6}/\text{yr}$. In all our calculations, unlimited solubility limits were used except for U, which was assumed to be very low.

SKB's deterministic calculation for the nominal corrosion scenario (i.e., SNF degradation rate of 1×10^{-7} /yr) showed a peak NF DER of 22 $\mu\text{Sv/yr}$ at canister failure time of $\sim 115,000$ years, and FF DER of 3.2 $\mu\text{Sv/yr}$ at 600,000 years.

Our deterministic calculation with SNF degradation rate of 1×10^{-7} /yr showed a peak NF DER of 36.17 $\mu\text{Sv/yr}$ at 115,200 years and FF DER of 5.47 $\mu\text{Sv/yr}$ at 630,000 years, which compared well with SKB's. Results match within a factor of 2. This calculation was done to first understand the difference between our model and the SKB model before calculating the effect of faster degradation rate using our model.

SKB's probabilistic calculation for the nominal corrosion case shows a mean peak NF and FF DERs of .59 $\mu\text{Sv/yr}$ and .18 $\mu\text{Sv/yr}$, respectively, both occurring at 1,000,000 years. For NF release, Ra-226, Pb-210, and Np-237 were dominant radionuclides whereas for FF release Ra-226, I-129, and Np-237 were the dominant radionuclides,

Our probabilistic calculation (100 realizations) showed a peak NF DER of 0.131 $\mu\text{Sv/yr}$ at 955,000 years and an FF DER of 0.118 occurring at 1,000,000 years. Np-237, Th-230, and I-129 were the main NF DER contributors whereas for FF DER, Ra-226 was the major contributor followed by I-129 and Np-237. We are able to match the sequence of radionuclides contributing to DER when we assign low solubility limit to Th and U instead of just U. In this case, our calculation shows a peak NF DER of 0.84 $\mu\text{Sv/yr}$ at 1,000,000 years and FF DER of .37 at 1,000,000 years.

When the SNF degradation rate was increased by an order of magnitude, for the deterministic case, our calculation showed an increase in the peak NF DER to 68.9 $\mu\text{Sv/yr}$ at 115,200 years and a FF DER of 38.8 $\mu\text{Sv/yr}$ at 610,000 years. Fig. 8 shows the effect of the faster degradation rate on the NF and FF DERs.

For the probabilistic run, we shifted the log-triangular distribution for SNF degradation rate by a factor of 10 toward higher values. Our calculations showed a peak NF DER of 0.91 $\mu\text{Sv/yr}$ at 730,000 years and FF DER of 1.16 $\mu\text{Sv/yr}$ at 975,000 years. The FF DER is approximately an order of magnitude higher than the nominal SNF degradation case. The primary contributors to DER remained the same. Thus a change of the degradation rate by one order of magnitude resulted in one order of magnitude increase in the FF DER. The analysis showed a linear relationship between the degradation rate and the FF DER.

3. The Consultants' overall assessment

3.1. Motivation of the assessment

The motivation for this work was to provide insights into SKB's implementation of what-if analysis and its barrier function demonstration. We addressed the technical review assignment by carrying out the following tasks: (i) developing a simple model to test SKB's demonstration of the retarding capacity of the waste form, buffer, backfill, and geosphere, that is suitable for exploring uncertainties and sensitivities related to these repository subsystems, (ii) approximating SKB results for a few example cases, (iii) exercising a what-if calculational case different from SKB's, and (iv) identifying any potential shortcomings in the safety case based on the limited calculations and verifications.

3.2. The Consultants' assessment

3.2.1. Assessment of the SKB Documentation

Our conclusions are that by and large, SKB described its modelling approach and computations in a manner that is sufficiently transparent for independent reproduction. Based on our limited analyses, SKB's "what if" cases (which are variants to the main scenarios and residual scenarios for conducting sensitivity analyses and illustrating "barrier functions) are reasonable. SKB clearly stated where parameter values or model assumptions are pessimistic or hypothetical. SKB reported several what-if cases in which barrier functions have been neutralized (i.e., no protection from a particular barrier). Loss of barrier functions are limited to the growing pinhole failure residual case. SKB characterizes all residual scenarios and what-if (or barrier-loss) cases derived from them as 'hypothetical' scenarios, implying that such scenarios are unlikely to happen. However, the pessimistic assumptions made in the main scenarios (e.g., no geosphere protection in the shear load case) can be construed as barrier loss cases though SKB does not categorize any calculations that are variants of the main scenarios as the barrier function loss calculations.

A reasonable set of what-if cases was considered by SKB, but it is not clear if a systematic approach (e.g., an enumeration of all possible combinations of selected degraded barrier components) was taken to develop what-if combinations for a comprehensive assessment. In several what-if cases, results were presented in a manner implying as if all what-if cases are either hypothetical or inconsequential. It would have been clearer if SKB had explained various aspects of a given scenario leading to a lower DER. For example SKB showed a relatively small change to the DER even if all canisters fail. But the fact that only a few canisters contribute to release in the calculation, even if all (or a large number of) canisters have failed, is not clearly stated and more detailed review is needed to understand this fact.

3.2.2. Assessment of calculations

We limited our quantitative analysis to developing a simplified model and testing the reproducibility of results for the main and residual scenarios. Exercising these scenarios helped us develop an understanding of the repository system's behaviour, which enabled us to discover shortcomings in the SKB model and identify aspects that may have not been considered by the SKB. We found relatively small differences between SKB results and our results. However, it should be noted that our models were constructed based on broad descriptions of the SKB models, seeking and implementing details only where strictly needed. It is likely that the differences can be reduced by understanding of flow fields SKB computed using detailed models, and flow correlations in different parts of the system. We reasonably reproduced the SKB computations (within factors of five or less) with simplified models.

Our model for independent analysis includes various components SKB considered (Figs. 1 and 2) to the extent described in SKB's two main reports presenting what-if analysis results: TR-10-50 (SKB, 2010) and TR-11-01 (SKB, 2011). The independent analysis reproduces SKB results for the main scenarios (i.e., central corrosion and shear load) and residual scenarios (growing pinhole and isostatic load failures within a factor of 5 for both deterministic and probabilistic cases.

Our model was able to reproduce SKB's results for the initial-advection central-corrosion canister failure scenario case, which refers to early canister failure as a result of early advection, within a factor of 2, which is a reasonable match considering the independent sources of model development. Faster SNF degradation led to linear growth in the FF DER instead of exponential-type growth.

For the Growing Pinhole Case, our radionuclide release trends, radionuclides showing up as dominant, and the pathway release rates are similar and in most cases practically identical to SKB's, for both NF and FF, before and after 10,000 years. Thus, SKB results are reproducible for the Growing Pinhole Case. But with the data available in the Transport Report (SKB, 2010) and the Data Report (SKB, 2010a), we were able to reproduce the results from the deterministic pinhole case better than the probabilistic pinhole case.

For the crown-flow what-if scenario of the Growing Pinhole Case, our radionuclide-release trends are mostly identical to that of SKB's, both NF and FF and before and after 10,000 years. Our peak NF DER is within a factor of 2 and our FF DER is within a factor of 3 of SKB's results. Moreover, in our calculations Q1 release dominates over Q2 pathway release throughout the simulation period whereas in SKB's calculation the Q2 pathway release exceeds that of Q1 release most of the simulation period.

For the crown-flow what-if scenario of the pinhole case, we also re-analysed the fracture-tunnel intersection distance from the deposition hole location because it is not clear why SKB has selected a distance of 118 m instead of 5.1 m (used in the no-crown-flow case) for the hydrogeologic calculations and if SKB used 5.1 m as the median value for the intersection distance between the deposition hole and the Q3 fracture. Our calculation shows that the differences in the results of selecting 118 m or 5.1 m are small.

3.2.3. Overall assessment of the approach

We consider the what-if approach implemented by SKB to be generally reasonable. The cases SKB focused on in its analyses are reasonable, but it does not appear to have used a systematic method that exhaustively searches for key barrier-component combinations for estimating dose with respect to the regulatory threshold.

Some processes are not fully described by SKB, for example the relationship between the Q1, Q2, and Q3 flows, as well as parameters used in the probabilistic simulations (e.g., flow rates and fluxes, transport resistance parameters, and water travel times). Summarizing distributions used as input in the computations would enhance the transparency of the model implementation. In our computations, we applied a factor of 0.001 to the Ra solubility limit to emulate the SBK Ra releases. It is likely such a factor is associated with the concept of Ra-Ba co-precipitation. However, the solubility limits described in Appendix F of the Radionuclide Transport report presumably already included the Ra-Ba co-precipitation effect. Clarification on the precise solubility values used in the probabilistic computations is needed, as they influence results.

SKB concluded (see Section 13.11, in SKB TR-11-01) that the most pessimistic variants from the main corrosion scenario is at least an order of magnitude below the dose corresponding to the regulatory risk limit in 1,000,000 years. SKB's mean dose from the shear load scenario is ~2 orders of magnitude below the regulatory limit for 1,000,000 years. SKB's risk summation shows that the margin to compliance is ~1 order of magnitude when it pessimistically bounds a number of uncertainties in the risk calculation. In addition, our simplified model, which was developed primarily based on descriptions summarized in Figs. 1 and 2 and the associated descriptions in the SKB reports, reproduced results within a factor of 5 compared to SKB's results, suggesting that for the cases analysed, the results are not likely to exceed the dose risk limit.

However, further independent verifications are needed to determine if this conclusion holds true for a broader spectrum of what-if analyses.

- SKB's what-if analyses do not include cases involving the number of deposition holes along the flow paths. As a result, even when all canisters have failed in some what-if analysis cases the DER does not change significantly. Therefore, what-if analyses should be carried out in combinations with different number of deposition holes contributing to release.
- SKB's pinhole failure what-if analyses used only semi-correlated DFN for fluid flow. Fully-correlated or uncorrelated DFNs could lead to higher releases and therefore could be studied as what-if analysis cases.
- The spalling of the deposition hole primarily reduces the resistance to Q1 flow. It is not clear if the extent of spalling can be such that it will connect Q1 and Q2 pathways. What-if analyses could be carried out to investigate the release impact of these pathways as connected pathways.
- Investigations could continue to test the reproducibility of additional what-if cases presented by SKB, including SKB's additional hypothetical, residual cases and the cases in which SKB assumed that different barriers are completely lost. However, unlike SKB's calculations, alternative calculations could focus on determining the level of degradation of the barriers (including complete

degradation) that may lead to exceeding the dose limit, rather than solely focusing on the release that would result from a loss of a barrier.

- Flow fields, which control the transport in the deposition tunnel, need to be further analysed to develop a better understanding of SKB's use of the flow fields in the estimation of release through the Q3 release pathway.

4. References

Joyce S, Simpson T, Hartley L, Applegate D, Hoek J Jackson P, Swan D, Marsic N, Follin S, 2010. Groundwater flow modelling of periods with temperate climate conditions – Forsmark. SKB R-09-20, SvenskKärnbränslehantering AB.

Pensado, O., S. Mohanty. 2012. “Technical Note 2012:58 Independent Radionuclide Transport Modelling – Reproducing Results for Main Scenarios.” Stockholm, Sweden: Strål säkerhets myndigheten (SSM – Swedish Radiation Safety Authority).
<http://www.stralsakerhetsmyndigheten.se/Publikationer/Rapport/Avfall-transportfysiskt-skydd/2012/201258/>

Pensado, O., S. Mohanty, and P. LaPlante. “Verification of Calculational Cases In Performance Assessment for KBS-3 Repository.” Proceedings of the 2013 International High-Level Radioactive Waste Management Conference (IHLRWM), Albuquerque, New Mexico, April 29 – May 2, 2013. La Grange Park, Illinois: American Nuclear Society. 2013.

Pensado, O., S. Mohanty, and B. Sagar. 2014. Independent Modelling of Radionuclide Transport, Evaluation of Colloid Transport Modelling. Stockholm, Sweden: Strål säkerhets myndigheten (SSM – Swedish Radiation Safety Authority).

Selroos J-O, 2010. SR-Site groundwater flow modelling methodology, setup, and results. SKB R-09-22, SvenskKärnbränslehantering AB.

SKB, 2011. Long-term safety for the final repository at Forsmark: Main report of the SR-Site project. SKB TR-11-01, SvenskKärnbränslehantering AB.

SKB, 2010. Radionuclide transport report for the safety assessment SR-Site. SKB TR-10-50, SvenskKärnbränslehantering AB.

SKB, 2010a. Data report for the safety assessment SR-Site. SKB TR-10-52, SvenskKärnbränslehantering AB.

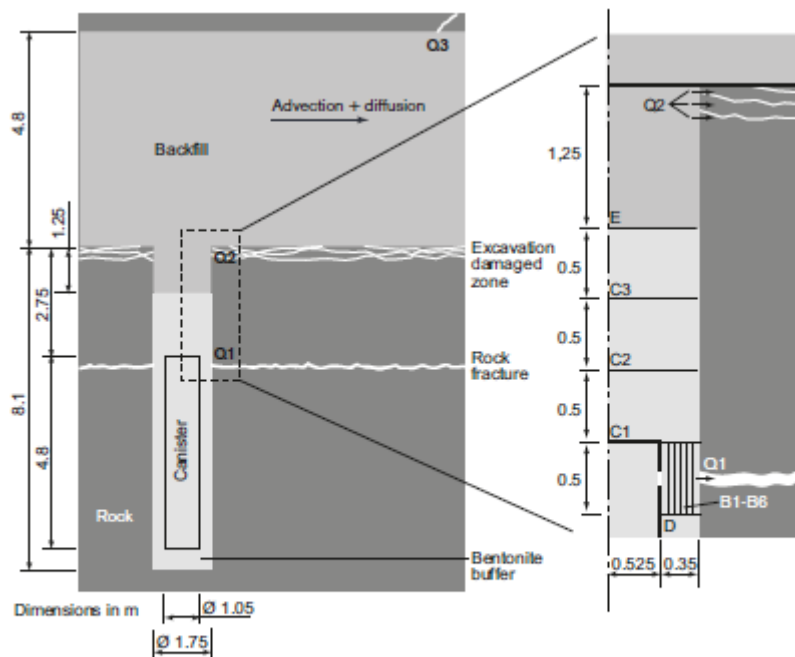


Figure G-3. Schematic picture of the compartments (including sub-compartments) B1-B6, C1-C3, D and E in the case with growing pinhole failure. The transport paths Q1, Q2 and Q3 to a fracture intersecting the deposition hole, to the excavation damaged zone, and to a fracture intersecting the deposition tunnel, respectively, are also shown.

Figure 1: Schematic showing the deposition hole and tunnel with dimensions (TR-10-50, pg. 300)

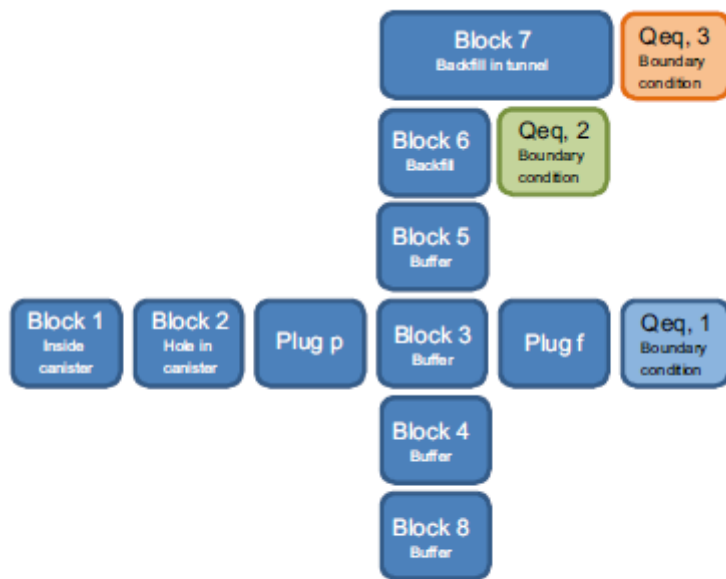


Figure G-2. Schematic picture of the blocks, plugs and boundary conditions in the case with growing pinhole failure without including the effect of spalling.

Figure 2: Schematic representation of SKB's model components for radionuclide transport for the case of Growing Pinhole Failure

Figure 3: Results of the verification modelling of the Growing Pinhole Canister failure scenario (top) contrasted with the corresponding SKB model results for the same cases, as presented in SKB's Radionuclide Transport Report: (a) to (d) deterministic run, (e) to (h) probabilistic run. The header of each figure at the top cites the corresponding SKB figure number from the Radionuclide Transport Report that is reproduced.

(a) Compares to Figure 6-11 of the Radionuclide Transport Report (Pinhole, Deterministic, NF)

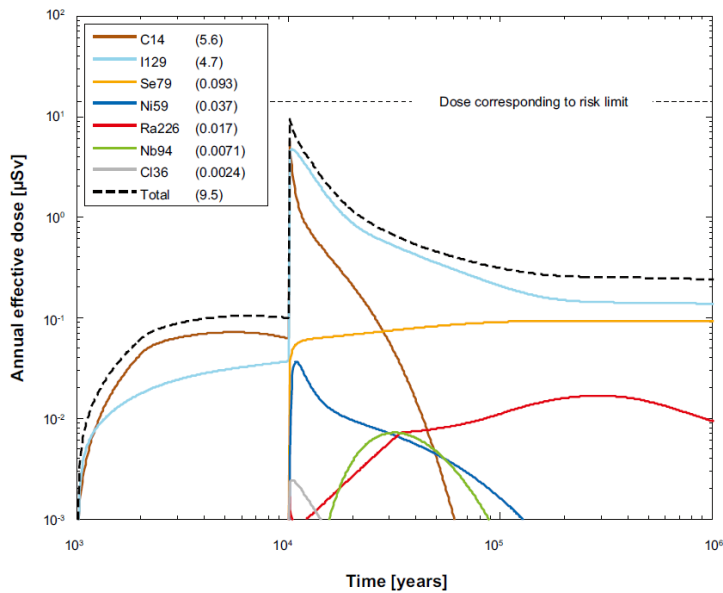
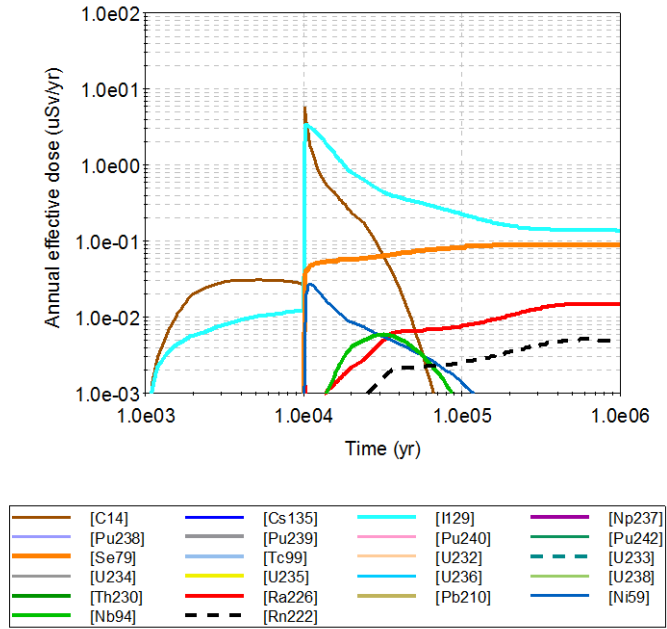


Figure 6-11. Near-field dose equivalent release for a deterministic calculation of the pinhole case, including the effect of spalling. Summed doses for all release paths (Q1+Q2+Q3). The legend is sorted by peak (in the one-million year period) of the annual effective dose. The values in brackets are peak dose in units of μSv .

(b) Compares to Figure 6-12 of the radionuclide transport report (pinhole, deterministic, NF)

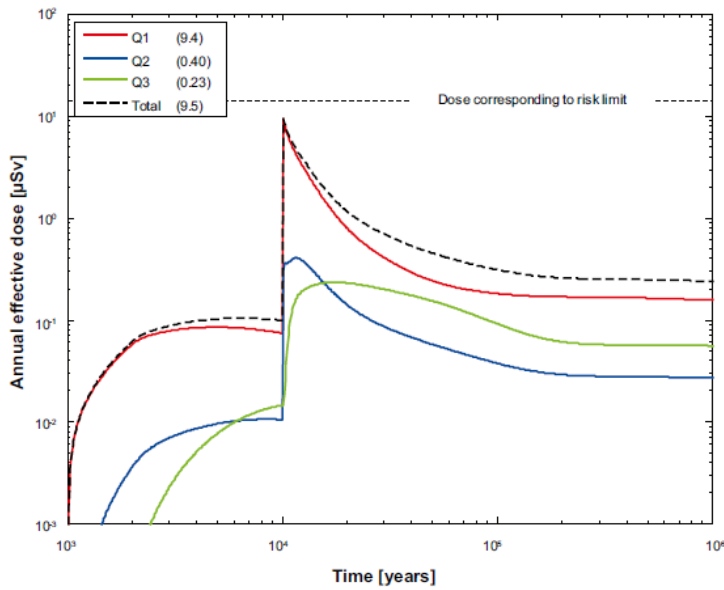
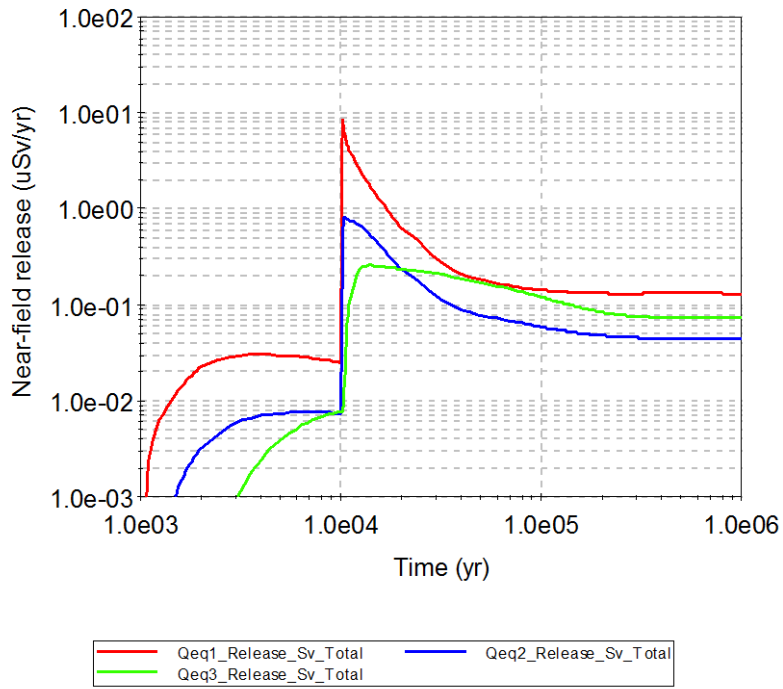


Figure 6-12. Near-field dose equivalent release for a deterministic calculation of the pinhole case, including the effect of spalling. Doses decomposed into Q1, Q2 and Q3. The legend is sorted by peak (in the one-million year period) of the annual effective dose. The values in brackets are peak dose in units of μSv .

(c) Compares to Figure 6-13 of the radionuclide transport report (pinhole, deterministic, NF)

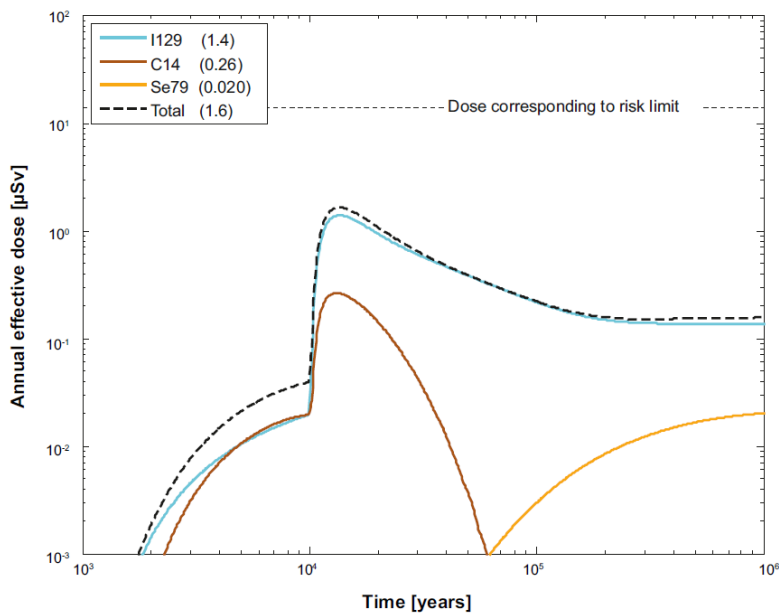
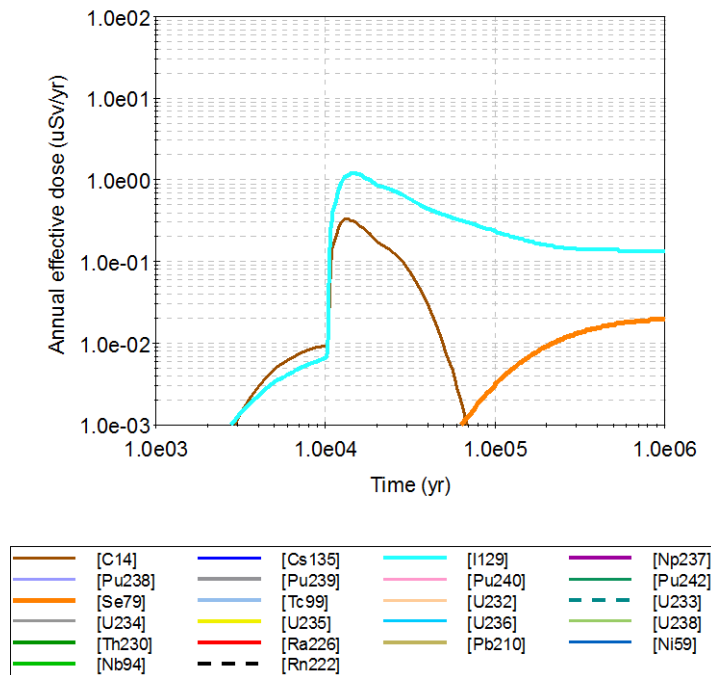


Figure 6-13. Far-field annual effective dose for a deterministic calculation of the pinhole case, including the effect of spalling. Summed doses for all release paths (Q1+Q2+Q3). The legend is sorted by peak (in the one-million year period) of the annual effective dose. The values in brackets are peak dose in units of μSv .

(d) Compares to Figure 6-14 of the radionuclide transport report (pinhole, deterministic, FF)

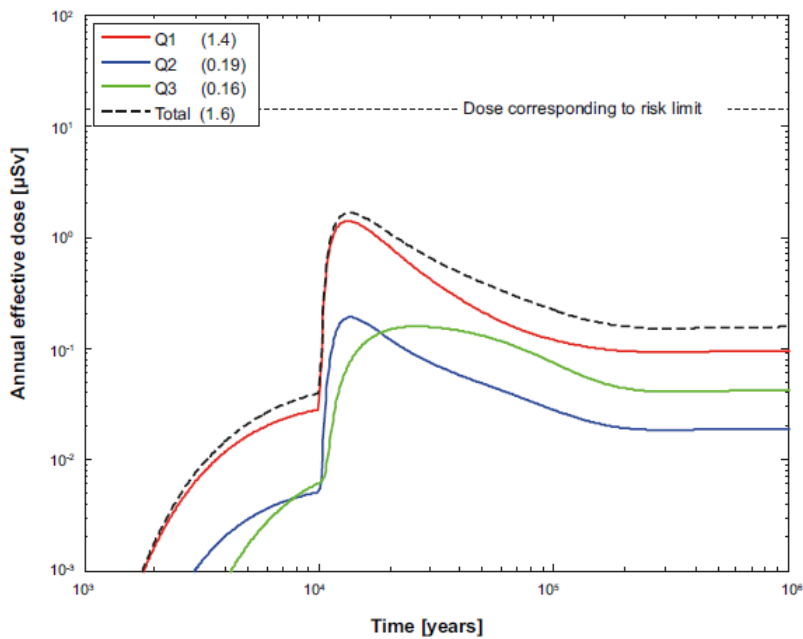
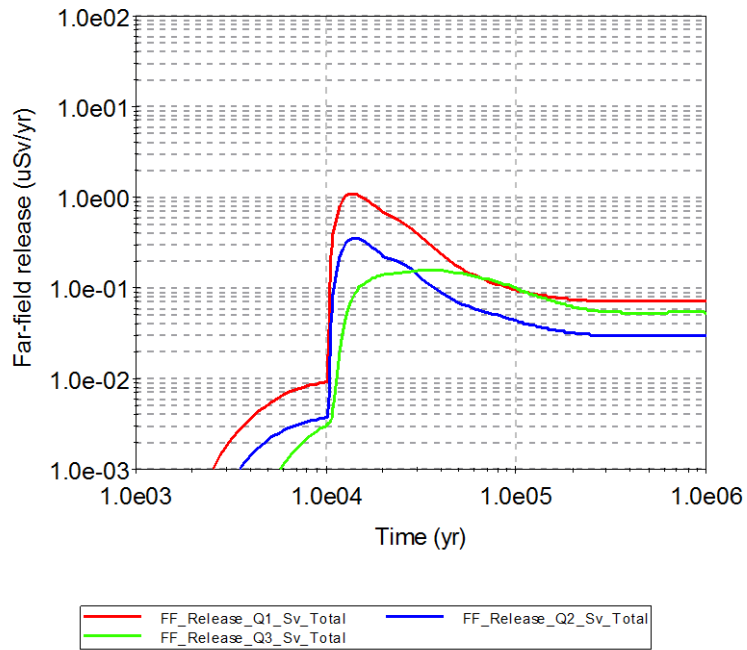
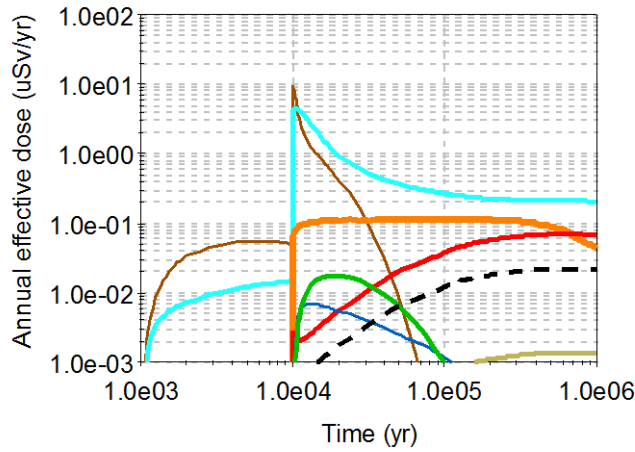


Figure 6-14. Far-field annual effective dose for a deterministic calculation of the pinhole case, including the effect of spalling. Doses decomposed into Q1, Q2 and Q3. The legend is sorted by peak (in the one-million year period) of the annual effective dose. The values in brackets are peak dose in units of μSv .

(e) Compares to Figure 6-15 of the radionuclide transport report (pinhole, probabilistic, NF)



[C14]	[Cs135]	[I129]
[Np237]	[Pu238]	[Pu239]
[Pu240]	[Pu242]	[Se79]
[Tc99]	[U232]	[U233]
[U234]	[U235]	[U236]
[U238]	[Th230]	[Ra226]
[Pb210]	[Ni59]	[Nb94]
[Rn222]		

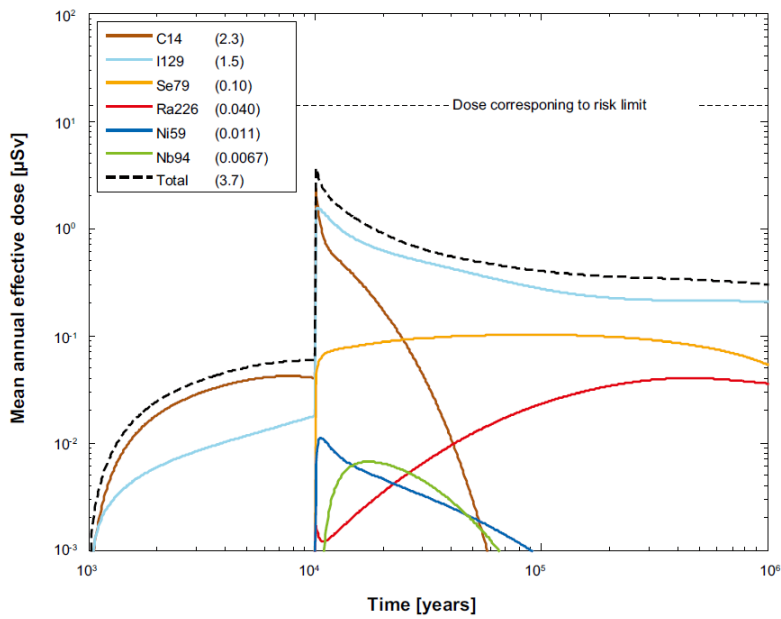


Figure 6-15. Near-field dose equivalent release for the probabilistic calculation of the pinhole case, including the effect of spalling. Summed doses for all release paths ($Q1+Q2+Q3$). The legend is sorted by peak (in the one-million year period) of the mean annual effective dose. The values in brackets are peak dose in units of μSv .

(f) Compares to Figure 6-16 of the radionuclide transport report–NF (pinhole, probabilistic, NF)

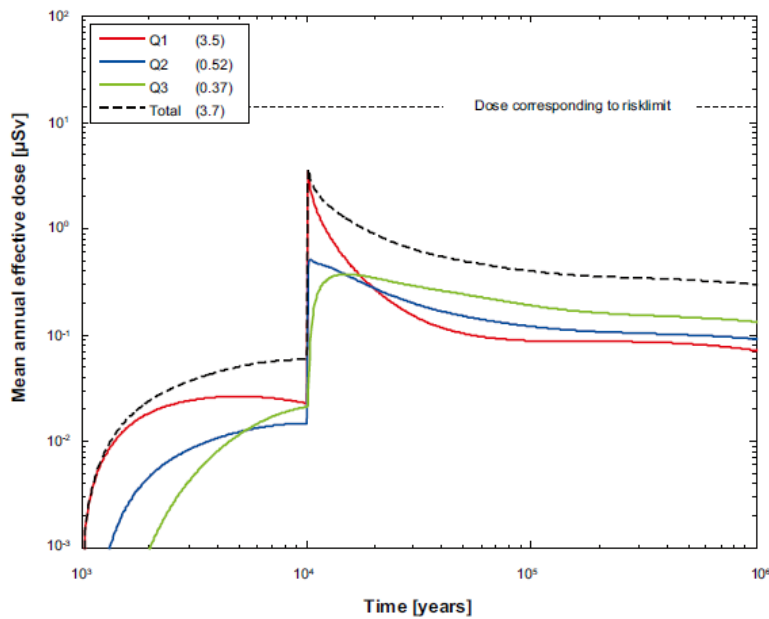
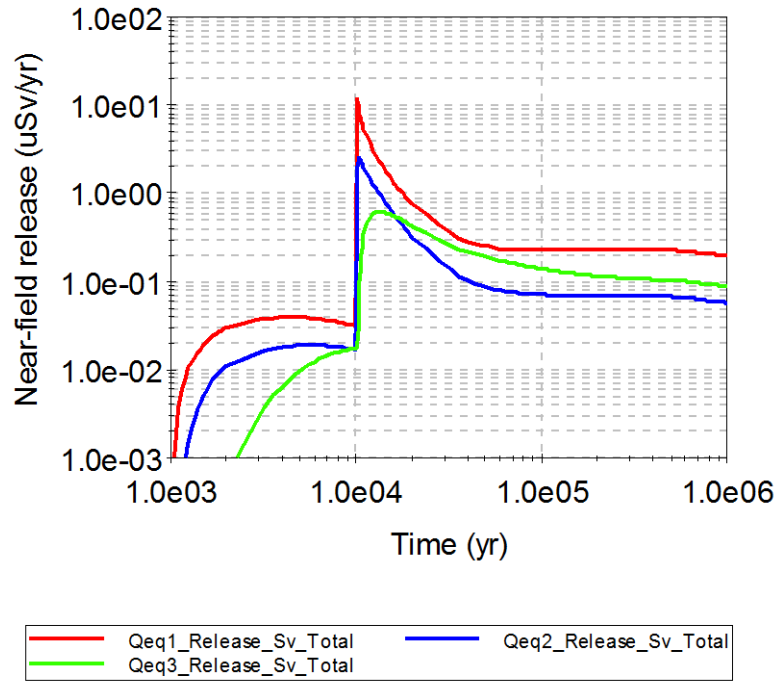


Figure 6-16. Near-field dose equivalent release for the probabilistic calculation of the pinhole case, including the effect of spalling. Doses decomposed into Q1, Q2 and Q3. The legend is sorted by peak (in the one-million year period) of the mean annual effective dose. The values in brackets are peak dose in units of μSv .

(g) Compares to Figure 6-17 of the radionuclide transport report (pinhole, probabilistic, FF)

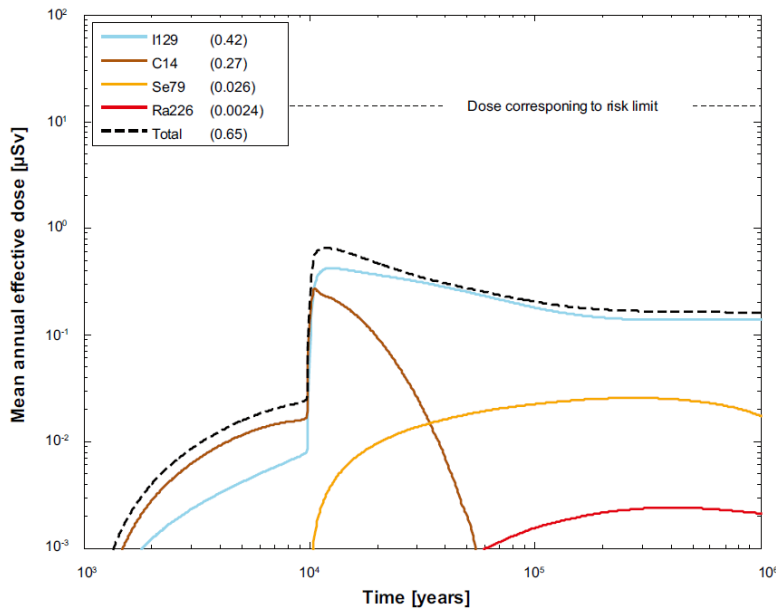
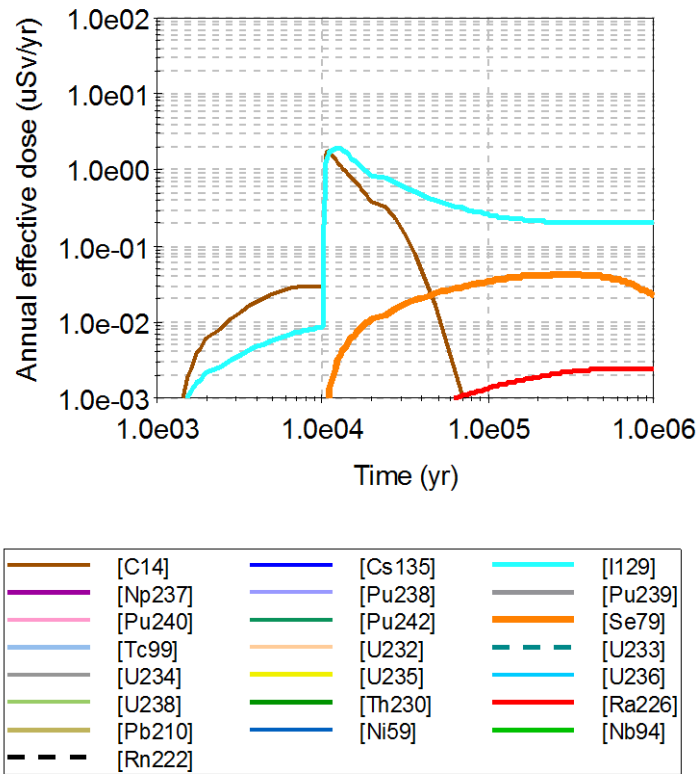


Figure 6-17. Far-field mean annual mean effective dose for the probabilistic calculation of the pinhole case, including the effect of spalling. Summed doses for all release paths (Q1+Q2+Q3). The legend is sorted by peak (in the one-million year period) of the mean annual effective dose. The values in brackets are peak dose in units of μSv .

(h) Compares to Figure 18 of the radionuclide transport report (pinhole, probabilistic, FF)

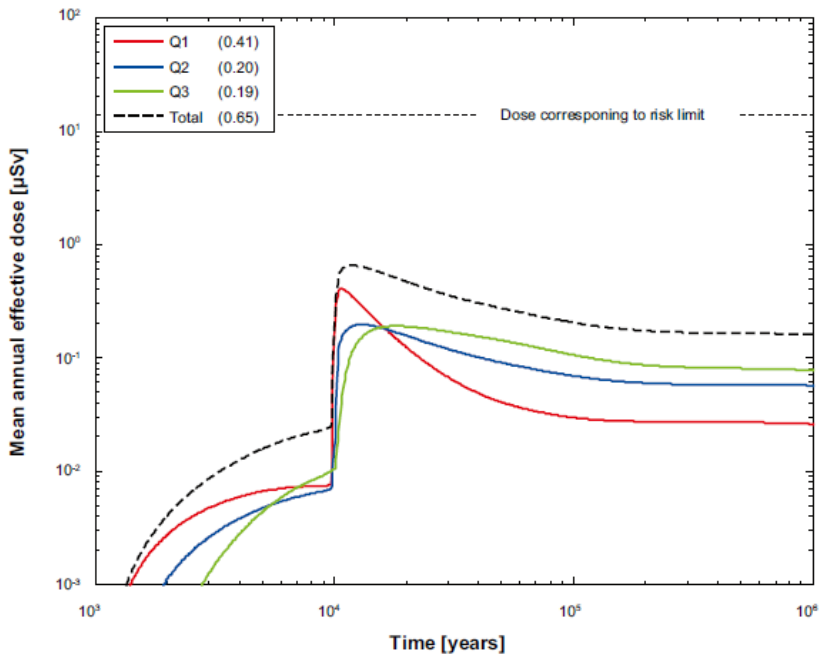
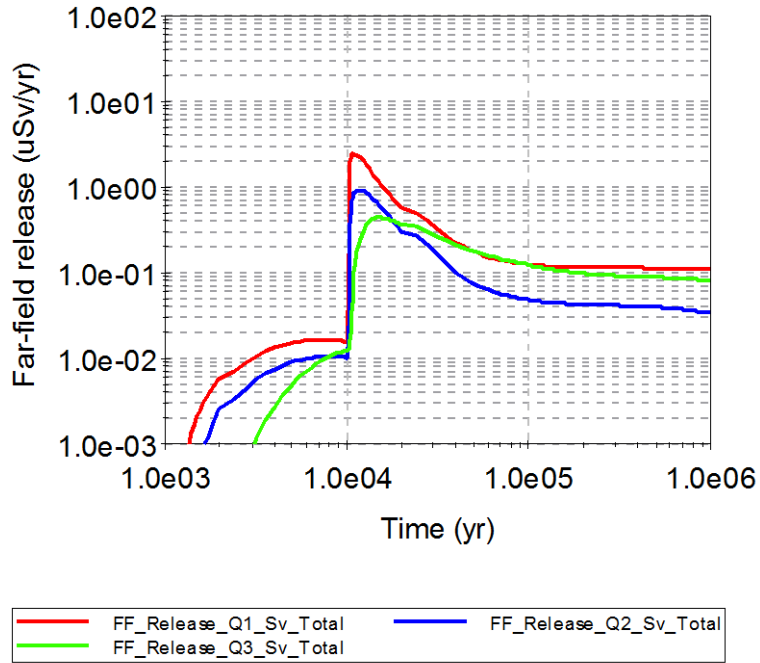


Figure 6-18. Far-field mean annual effective dose for the probabilistic calculation of the pinhole case, including the effect of spalling. Doses decomposed into Q1, Q2 and Q3. The legend is sorted by peak (in the one-million year period) of the mean annual effective dose. The values in brackets are peak dose in units of μSv .

Figure 4: Results of the verification modelling of the isostatic Load Failure scenario (top) contrasted with the corresponding SKB model results for the same case (i.e., the 10,000-years failure time case), as presented in SKB's Radionuclide Transport Report: (a) to (b) deterministic run, (c) to (d) probabilistic run. The header of each figure at the top cites the corresponding SKB figure number from the Radionuclide Transport Report that is reproduced at the top.

(a) Compares to Figure 6-1 of the Radionuclide Transport Report (Isostatic, Deterministic, NF)

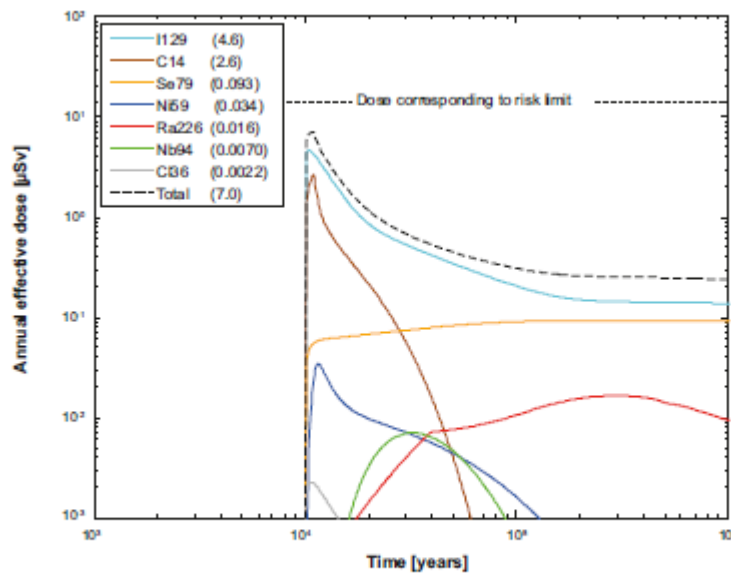
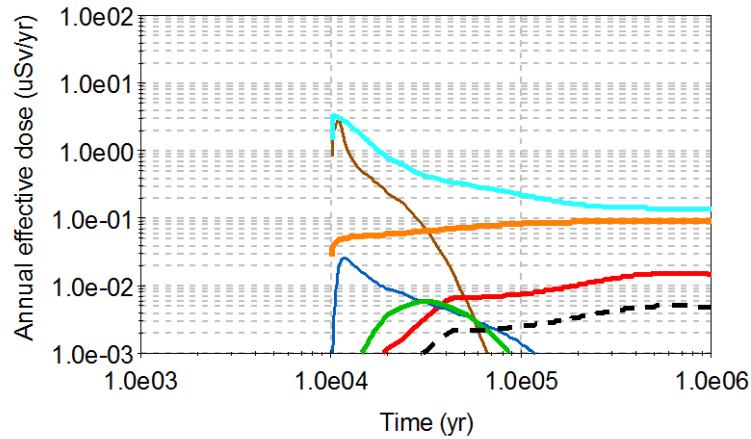
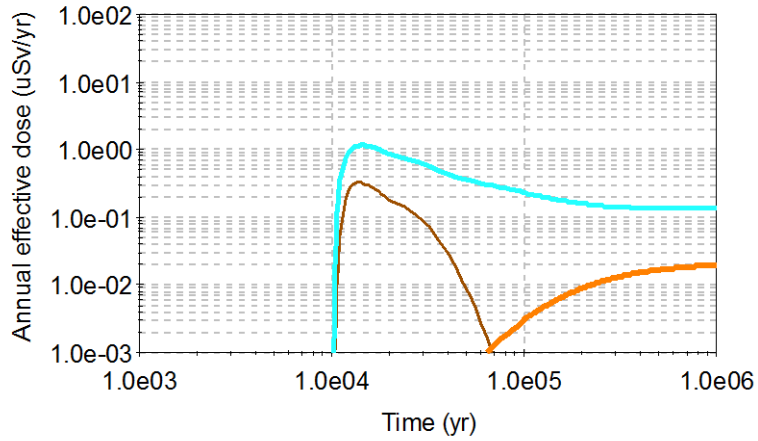


Figure 6-1. Near-field dose equivalent release for a deterministic calculation of the isostatic load scenario, with a postulated failure of one canister at 10,000 years. The legend is sorted by peak (in the one-million year period) of the annual effective dose. The values in brackets are peak dose in units of μSv .

(b) Compares to Figure 6-2 of the Radionuclide Transport Report (Isostatic, Deterministic, FF)



[C14]	[Cs135]	[I129]	[Np237]
[Pu238]	[Pu239]	[Pu240]	[Pu242]
[Se79]	[Tc99]	[U232]	[U233]
[U234]	[U235]	[U236]	[U238]
[Th230]	[Ra226]	[Pb210]	[Ni59]
[Nb94]	[Rn222]		

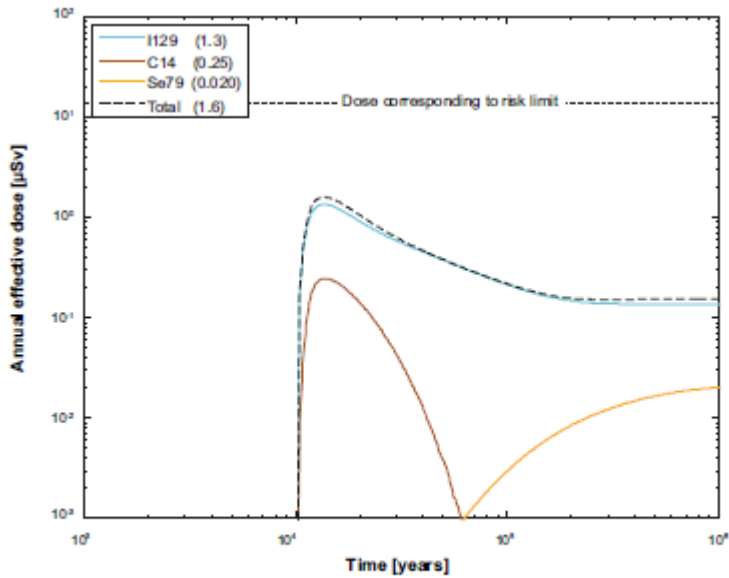
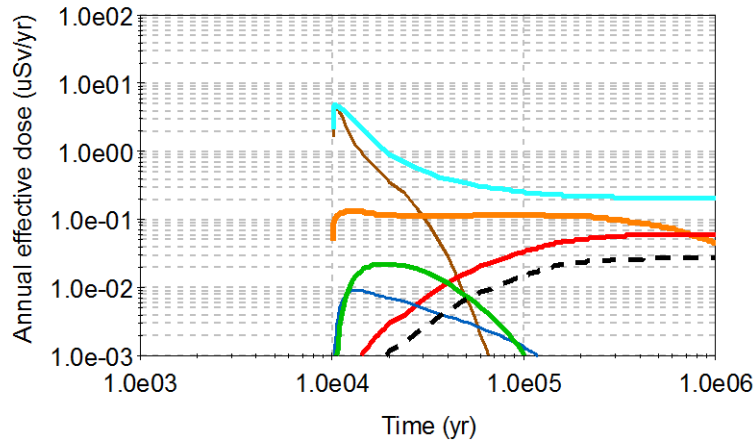


Figure 6-2. Far-field annual effective dose for a deterministic calculation of the isostatic load scenario, with a postulated failure of one canister at 10,000 years. The legend is sorted by peak (in the one-million year period) of the annual effective dose. The values in brackets are peak dose in units of μSv .

(c) Compares to Figure 6-3 of the Radionuclide Transport Report (Isostatic, probabilistic, NF)



[C14]	[Cs135]	[I129]	[Np237]
[Pu238]	[Pu239]	[Pu240]	[Pu242]
[Se79]	[Tc99]	[U232]	[U233]
[U234]	[U235]	[U236]	[U238]
[Th230]	[Ra226]	[Pb210]	[Ni59]
[Nb94]	[Rn222]		

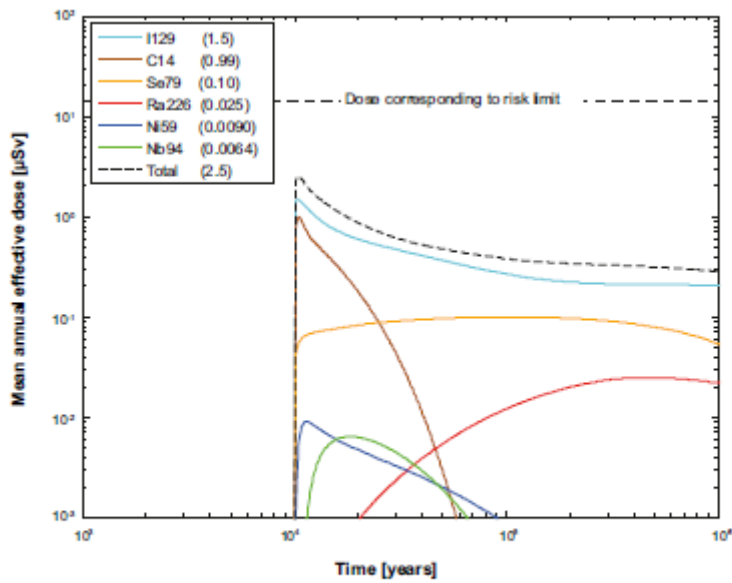


Figure 6-3. Near-field dose equivalent release for a probabilistic calculation of the isostatic load scenario, with a postulated failure of one canister at 10,000 years. The legend is sorted by peak (in the one-million year period) of the mean annual effective dose. The values in brackets are peak dose in units of μSv .

(d) Compares to Figure 6-4 of the Radionuclide Transport Report (Isostatic, Probabilistic, FF)

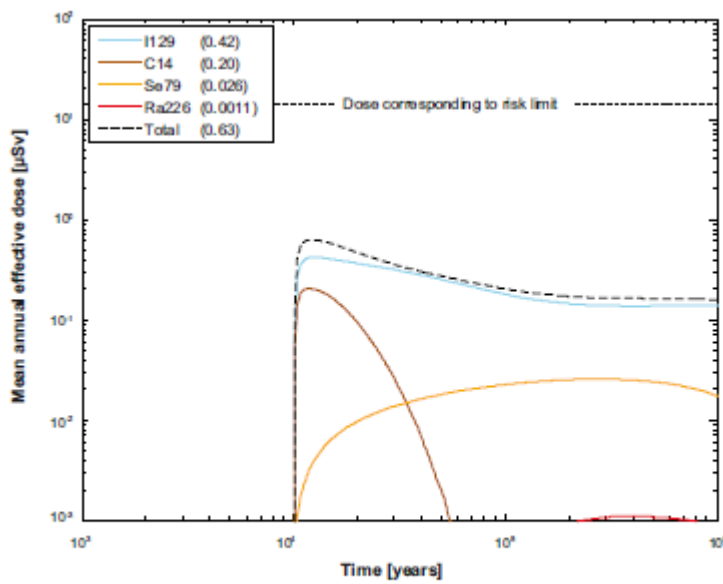
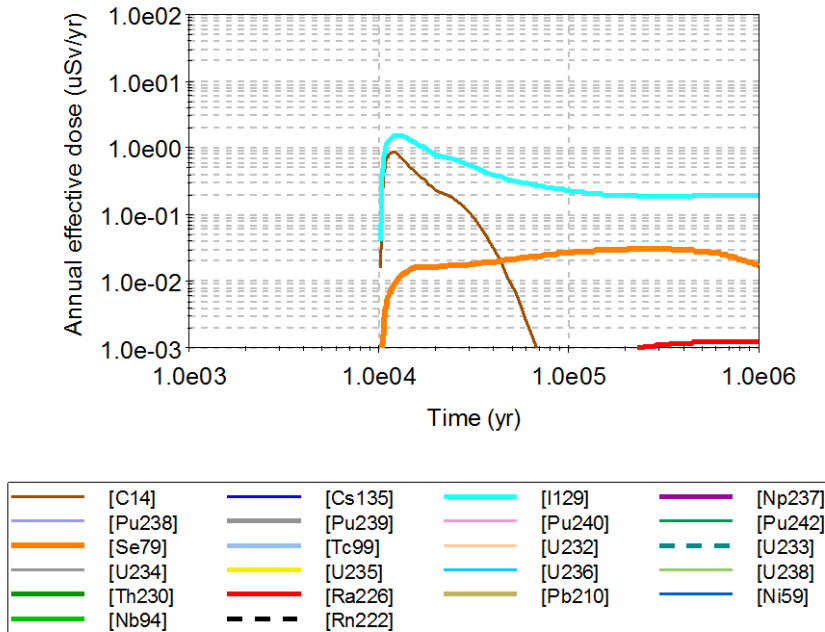


Figure 6-4. Far-field mean annual effective dose for a probabilistic calculation of the isostatic load scenario, with a postulated failure of one canister at 10,000 years. The legend is sorted by peak (in the one-million year period) of the mean annual effective dose. The values in brackets are peak dose in units of μSv .

Figure 5: Results of the verification modelling of the Growing Pinhole Failure + Crown Flow scenario (top) contrasted with the corresponding SKB model results for the same case, as presented in SKB's Radionuclide Transport Report: (a) deterministic run, (b) probabilistic run. The header of each figure at the top cites the corresponding SKB figure number from the Radionuclide Transport Report that is reproduced at the top.

(a): Compares to Figure 6-27 of the radionuclide transport report (crown flow, Deterministic, NF)

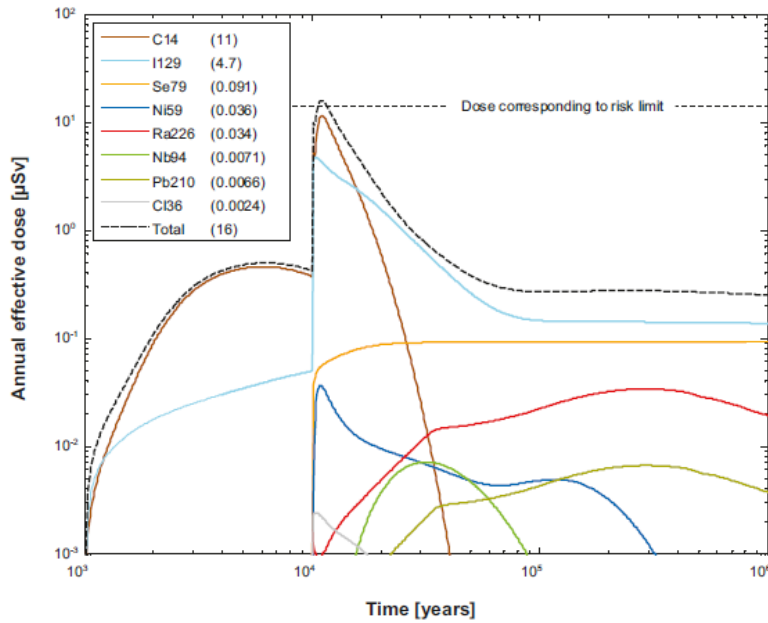
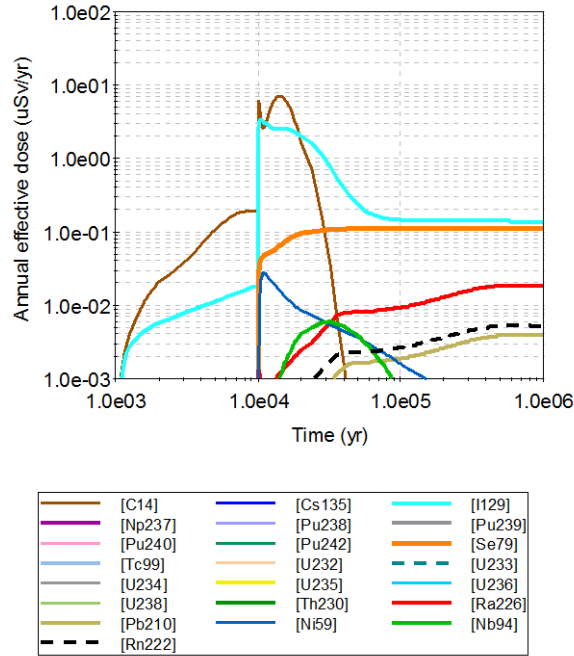


Figure 6-27. Near-field dose equivalent release for a deterministic calculation of the pinhole case, with lost swelling pressure in tunnel backfill. Summed doses for all release paths (Q1+Q2+Q3). The legend is sorted by peak (in the one-million year period) of the annual effective dose. The values in brackets are peak dose in units of μSv .

(b) Compares to Figure 6-28 of the Radionuclide Transport Report (crown flow, deterministic, NF)

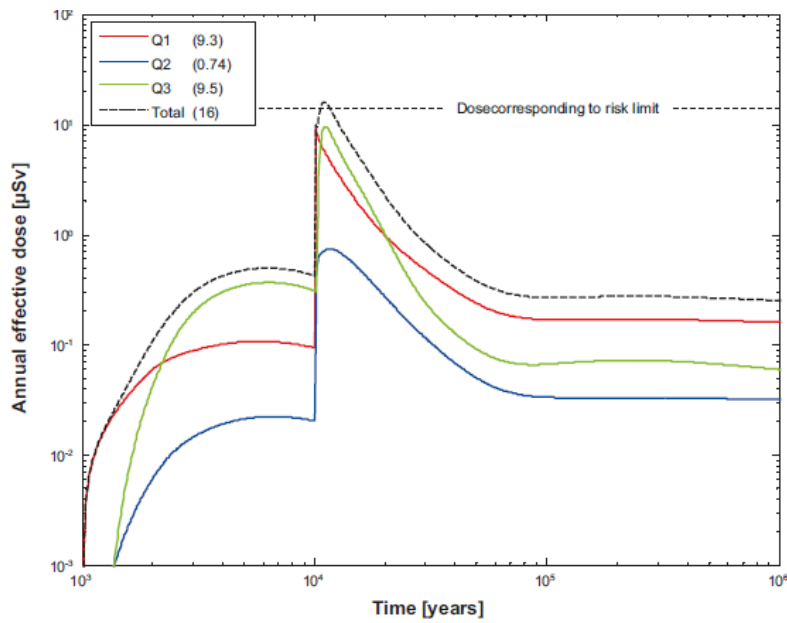
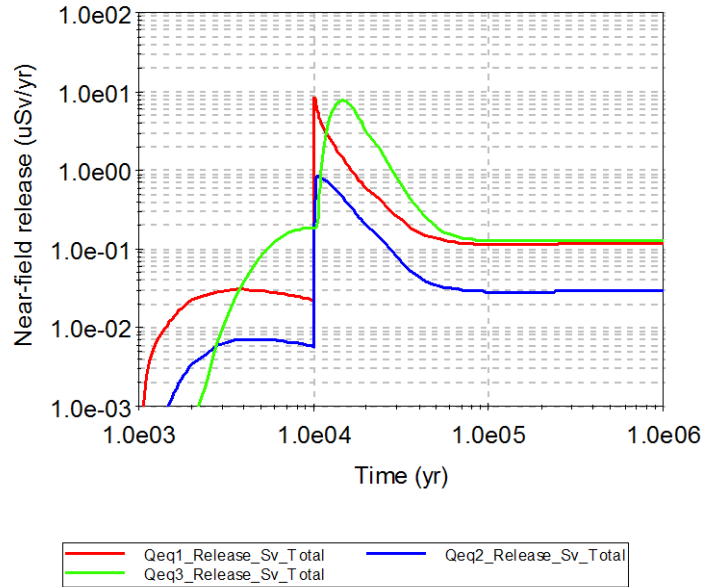


Figure 6-28. Near-field dose equivalent release for a deterministic calculation of the pinhole case, with lost swelling pressure in tunnel backfill. Doses decomposed into Q1, Q2 and Q3. The legend is sorted by peak (in the one-million year period) of the annual effective dose. The values in brackets are peak dose in units of μSv .

(c) Compares to Figure 6-29 of the Radionuclide Transport Report (crown flow, deterministic, FF)

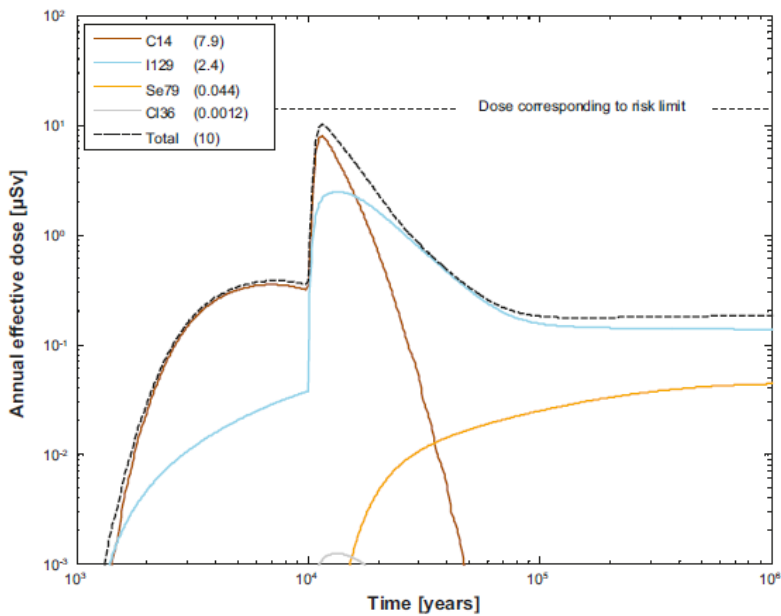
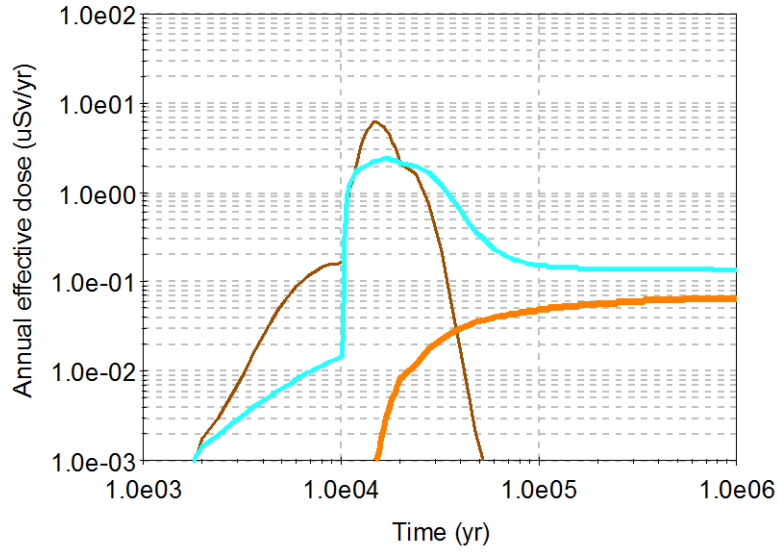


Figure 6-29. Far-field annual effective dose for a deterministic calculation of the pinhole case, with lost swelling pressure in tunnel backfill. Summed doses for all release paths (Q1+Q2+Q3). The legend is sorted by peak (in the one-million year period) of the annual effective dose. The values in brackets are peak dose in units of μSv .

(d) Compares to Figure 6-30 of the Radionuclide Transport Report (crown flow, deterministic, FF)

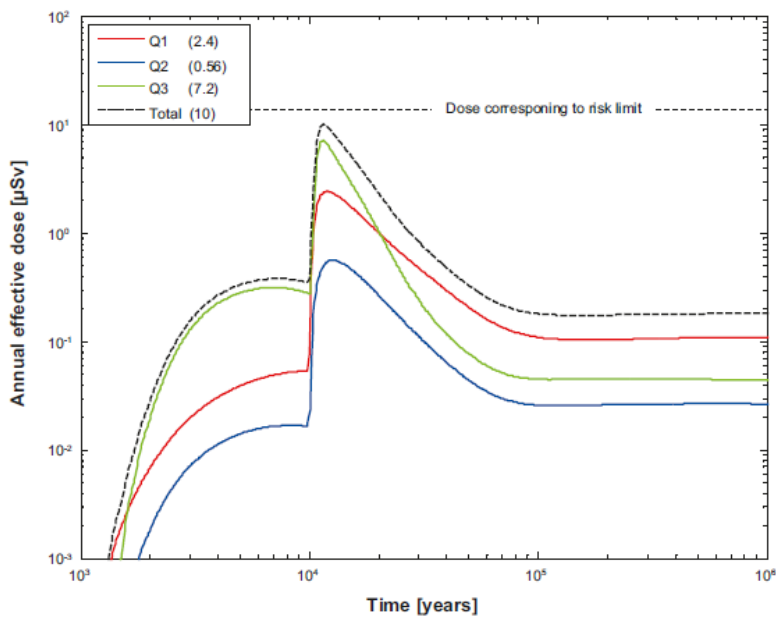
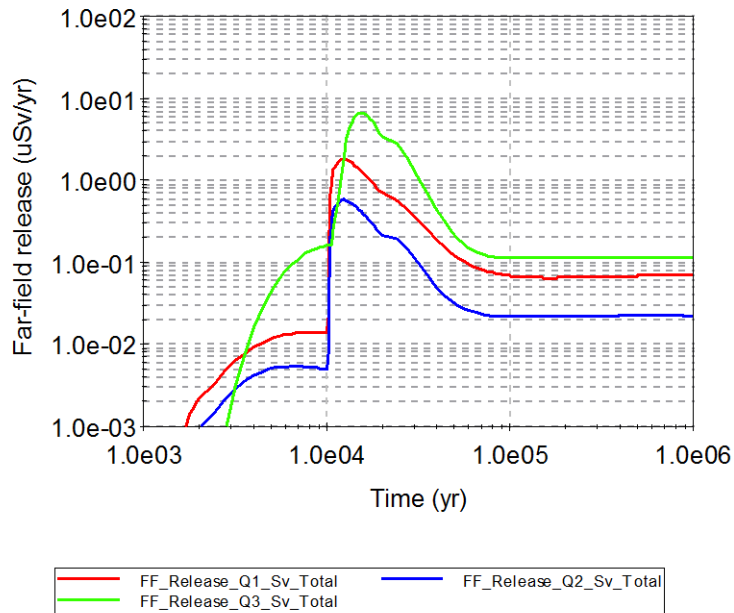


Figure 6-30. Far-field annual effective dose for a deterministic calculation of the pinhole case, with lost swelling pressure in tunnel backfill. Doses decomposed into Q1, Q2 and Q3. The legend is sorted by peak (in the one-million year period) of the annual effective dose. The values in brackets are peak dose in units of μSv .

(e) Compares to Figure 6-31 of the Radionuclide Transport Report (crown flow, probabilistic, NF)

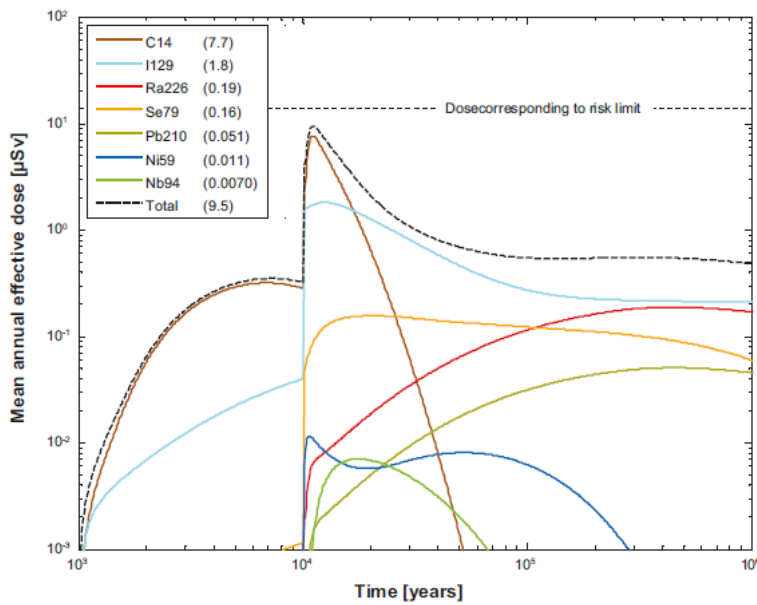
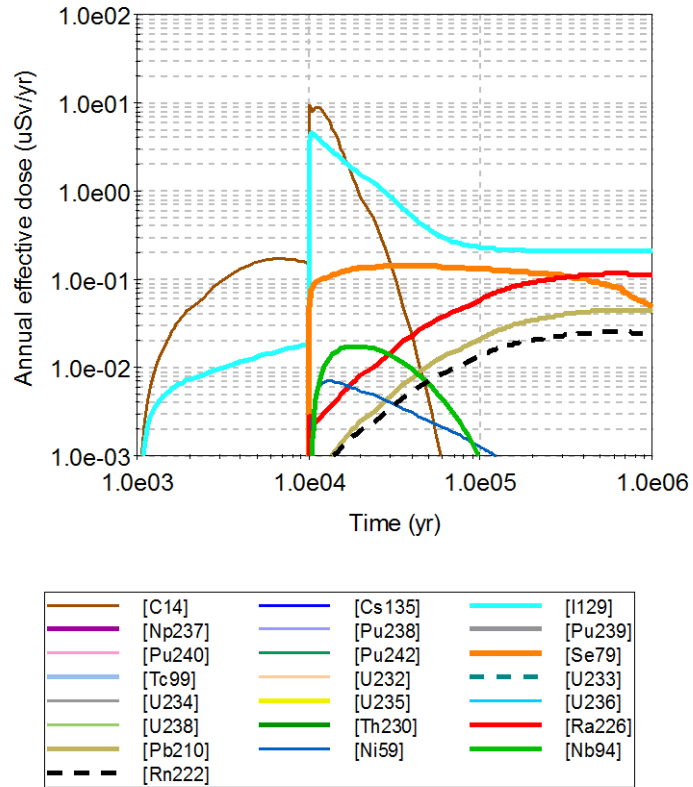


Figure 6-31. Near-field dose equivalent release for the probabilistic calculation of the pinhole case, with lost swelling pressure in tunnel backfill. Summed doses for all release paths ($Q_1+Q_2+Q_3$). The legend is sorted by peak (in the one-million year period) of the mean annual effective dose. The values in brackets are peak dose in units of μSv .

(f) Compares to Figure 6-32 of the Radionuclide Transport Report (crown flow, probabilistic, NF)

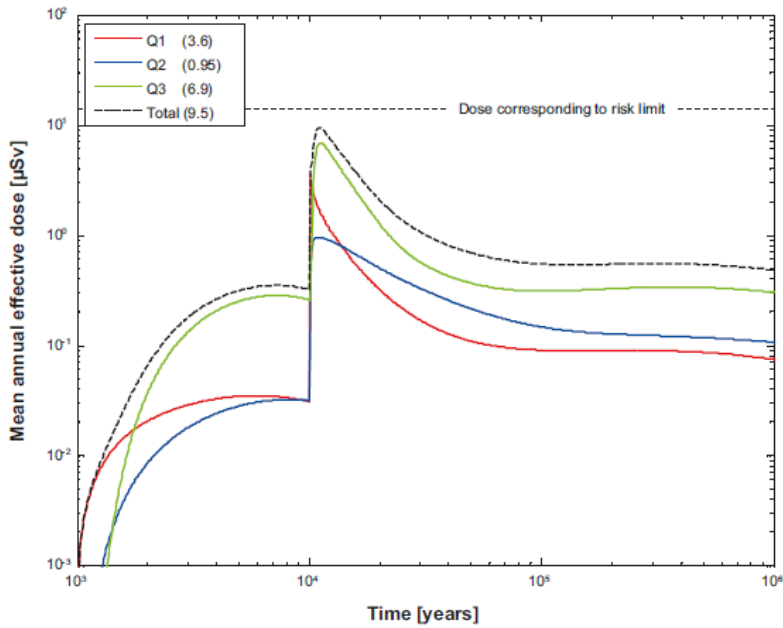
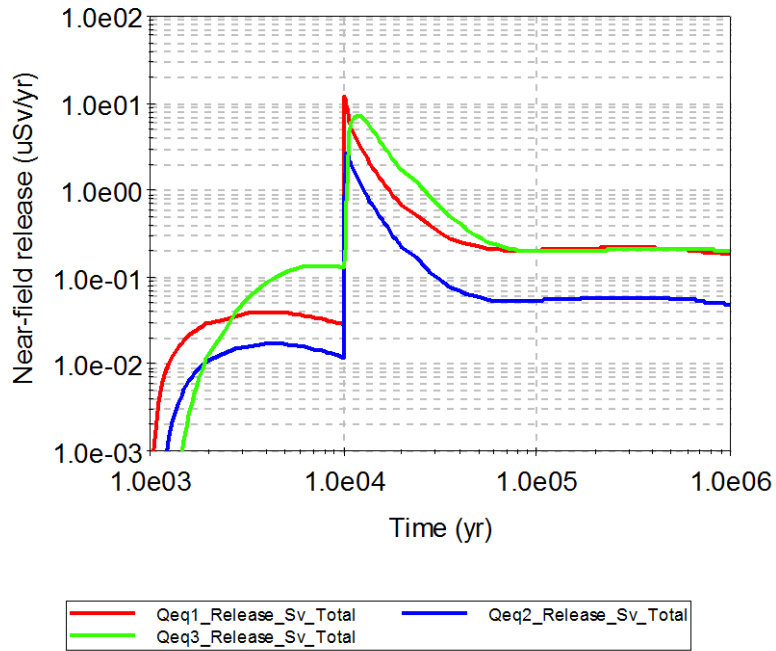
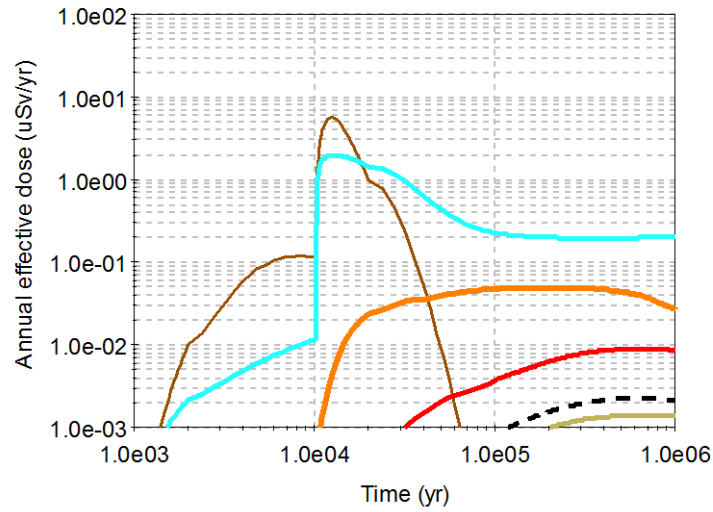


Figure 6-32. Near-field dose equivalent release for the probabilistic calculation of the pinhole case, with lost swelling pressure in tunnel backfill. Doses decomposed into Q1, Q2 and Q3. The legend is sorted by peak (in the one-million year period) of the mean annual effective dose. The values in brackets are peak dose in units of μSv .

(g) Compares to Figure 6-33 of the Radionuclide Transport Report (crown flow, probabilistic, FF)



[C14]	[Cs135]	[I129]	[Np237]
[Pu238]	[Pu239]	[Pu240]	[Pu242]
[Se79]	[Tc99]	[U232]	[U233]
[U234]	[U235]	[U236]	[U238]
[Th230]	[Ra226]	[Pb210]	[Ni59]
[Nb94]	[Rn222]		

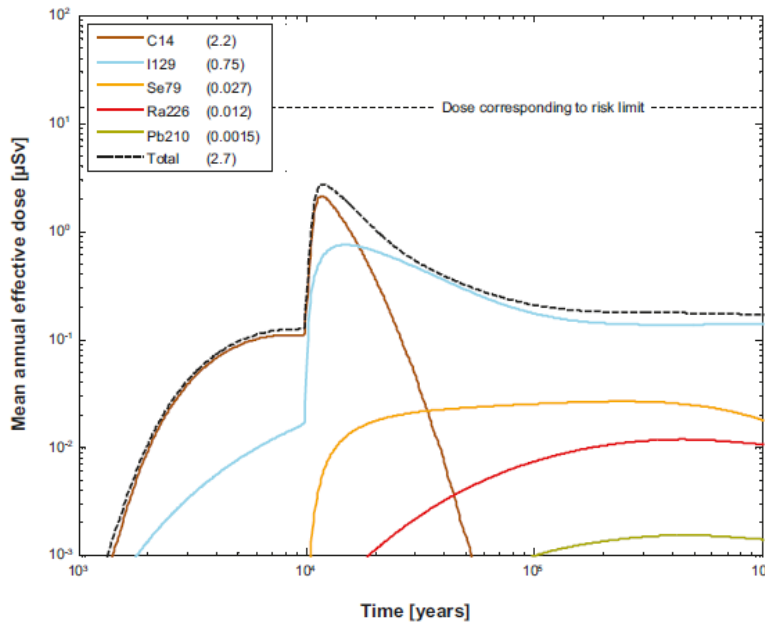


Figure 6-33. Far-field mean annual mean effective dose for the probabilistic calculation of the pinhole case, with lost swelling pressure in tunnel backfill. Summed doses for all release paths ($Q1+Q2+Q3$). The legend is sorted by peak (in the one-million year period) of the mean annual effective dose. The values in brackets are peak dose in units of μSv .

(h) Compares to Figure 6-34 of the Radionuclide Transport Report (crown flow, probabilistic, FF)

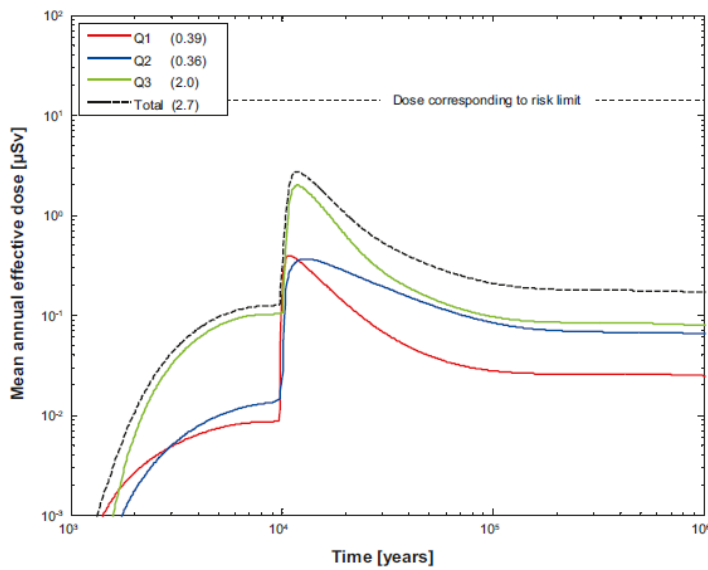
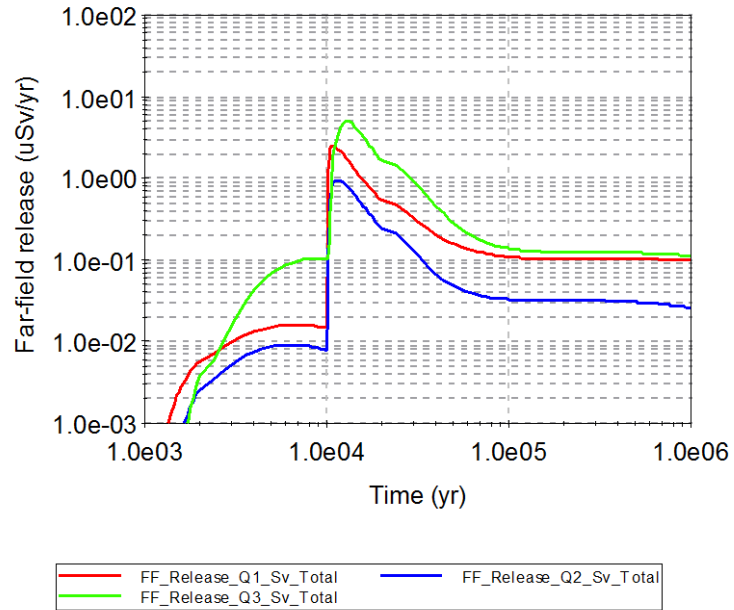


Figure 6-34. Far-field mean annual effective dose for the probabilistic calculation of the pinhole case, with lost swelling pressure in tunnel backfill. Doses decomposed into Q1, Q2 and Q3. The legend is sorted by peak (in the one-million year period) of the mean annual effective dose. The values in brackets are peak dose in units of μSv .

Figure 6: Results of the verification modelling of corrosion failure scenario with initial advection

(a) Compares to Figure 4-28 of the Radionuclide Transport Report (corrosion, initial advection, deterministic, NF)

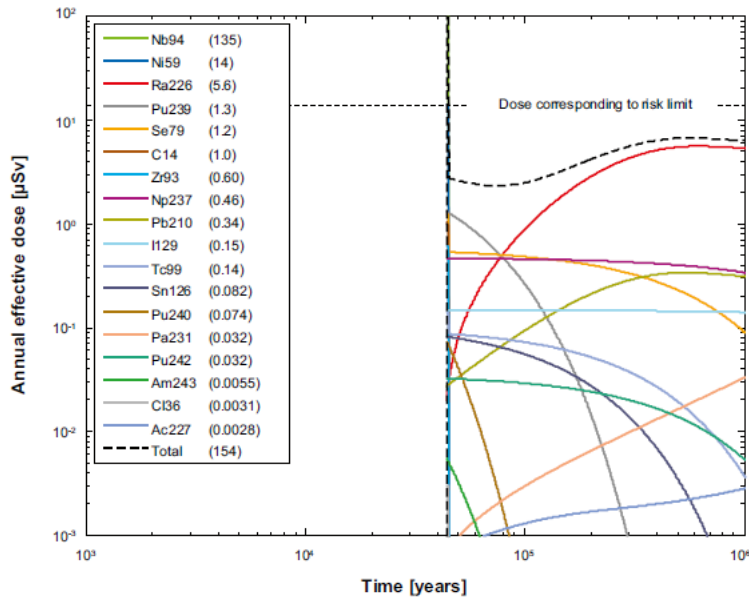
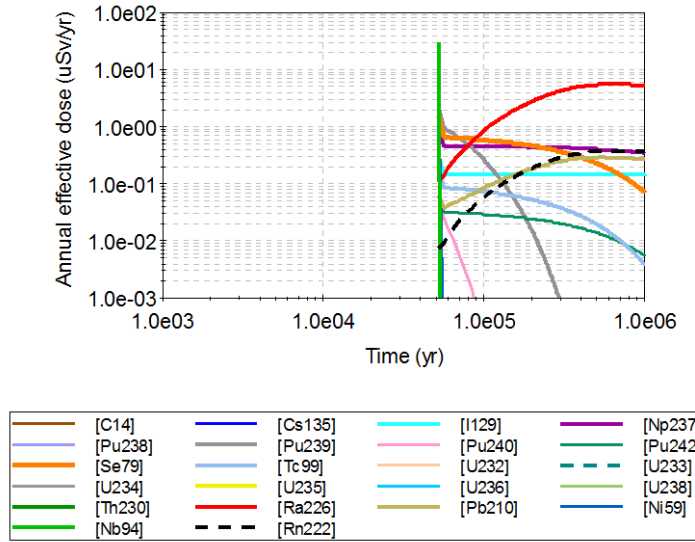
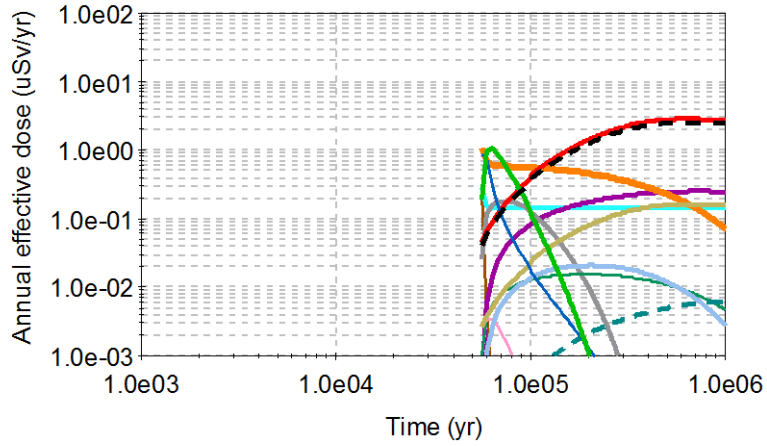


Figure 4-28. Near-field dose equivalent release for a deterministic calculation of the central corrosion case, with initial advection in the erosion/corrosion model. The legend is sorted by peak (in the one-million year period) of the annual effective dose. The values in brackets are peak dose in units of μSv . Note that the dose equivalent release for Nb-94 is 135 $\mu\text{Sv}/\text{year}$, i.e. above the limit of the y-axis.

(b) Compares to Figure 4-29 of the Radionuclide Transport Report (corrosion, initial advection, deterministic, FF)



[C14]	[Cs135]	[I129]	[Np237]
[Pu238]	[Pu239]	[Pu240]	[Pu242]
[Se79]	[Tc99]	[U232]	[U233]
[U234]	[U235]	[U236]	[U238]
[Th230]	[Ra226]	[Pb210]	[Ni59]
[Nb94]	[Rn222]		

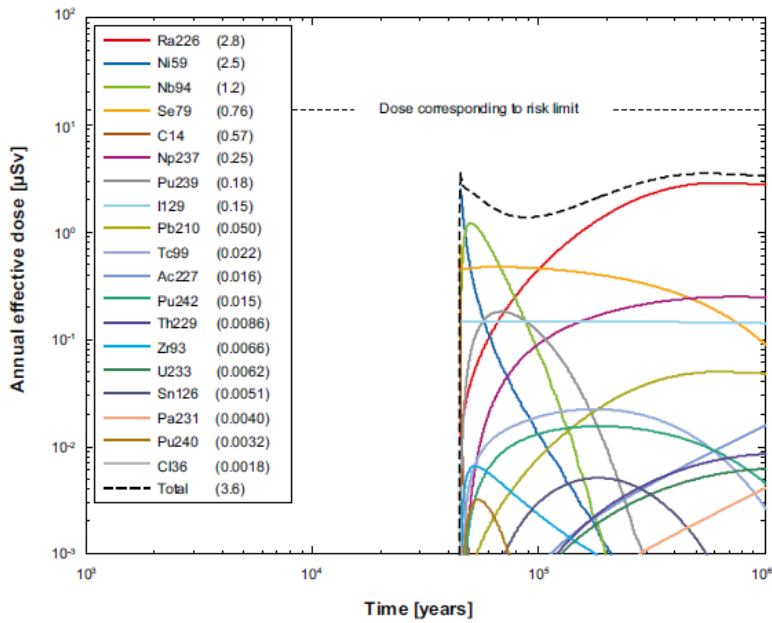
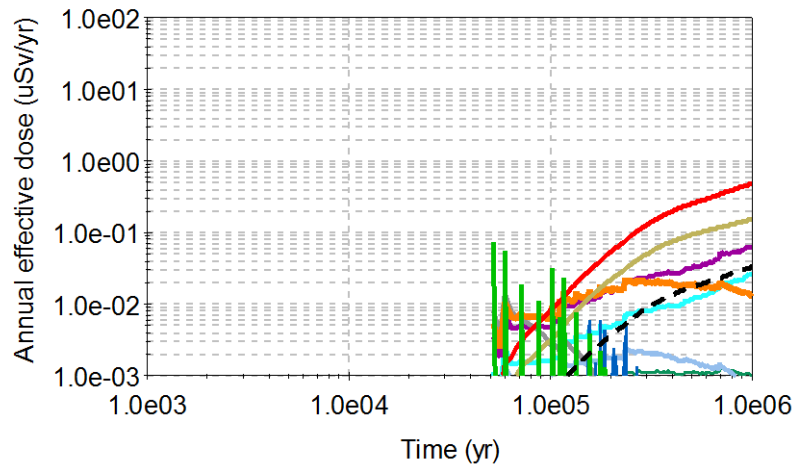


Figure 4-29. Far-field annual effective dose for a deterministic calculation of the central corrosion case, with initial advection in the erosion/corrosion model. The legend is sorted by peak (in the one-million year period) of the annual effective dose. The values in brackets are peak dose in units of μSv .

(c) Compares to Figure 4-30 of the Radionuclide Transport Report (corrosion, initial advection, probabilistic, NF)



[C14]	[Cs135]	[I129]	[Np237]
[Pu238]	[Pu239]	[Pu240]	[Pu242]
[Se79]	[Tc99]	[U232]	[U233]
[U234]	[U235]	[U236]	[U238]
[Th230]	[Ra226]	[Pb210]	[Ni59]
[Nb94]	[Rn222]		

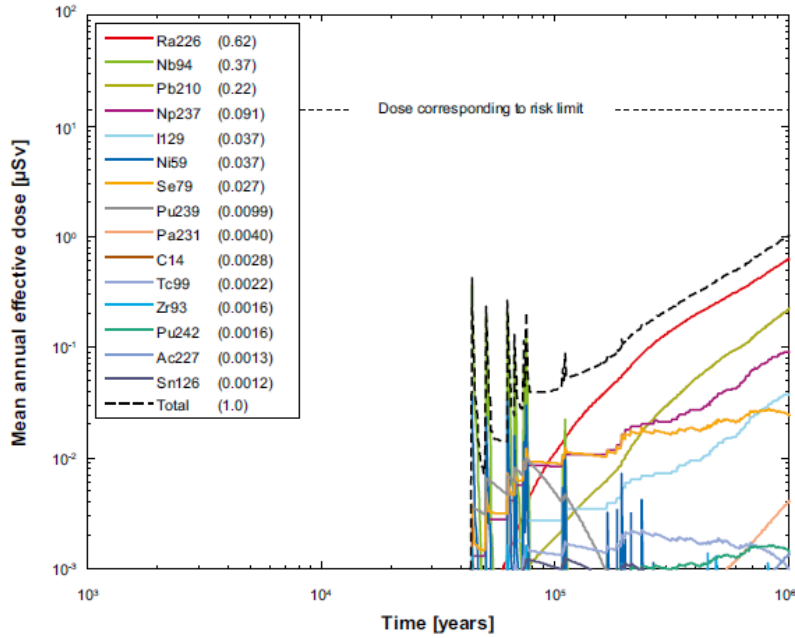
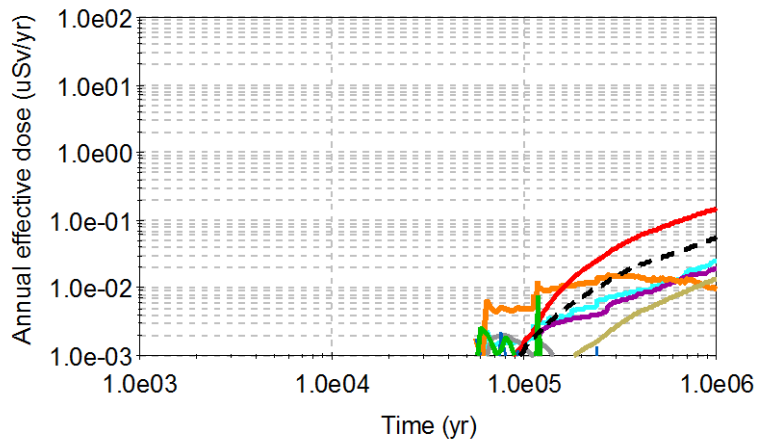


Figure 4-30. Near-field dose equivalent release for a probabilistic calculation of the central corrosion case, with initial advection in the erosion/corrosion model. The legend is sorted by peak (in the one-million year period) of the mean annual effective dose. The values in brackets are peak dose in units of μSv .

(d) Compares to Figure 4-31 of the Radionuclide Transport Report (corrosion, initial advection, probabilistic, FF)



[C14]	[Cs135]	[I129]	[Np237]
[Pu238]	[Pu239]	[Pu240]	[Pu242]
[Se79]	[Tc99]	[U232]	[U233]
[U234]	[U235]	[U236]	[U238]
[Th230]	[Ra226]	[Pb210]	[Ni59]
[Nb94]	[Rn222]		

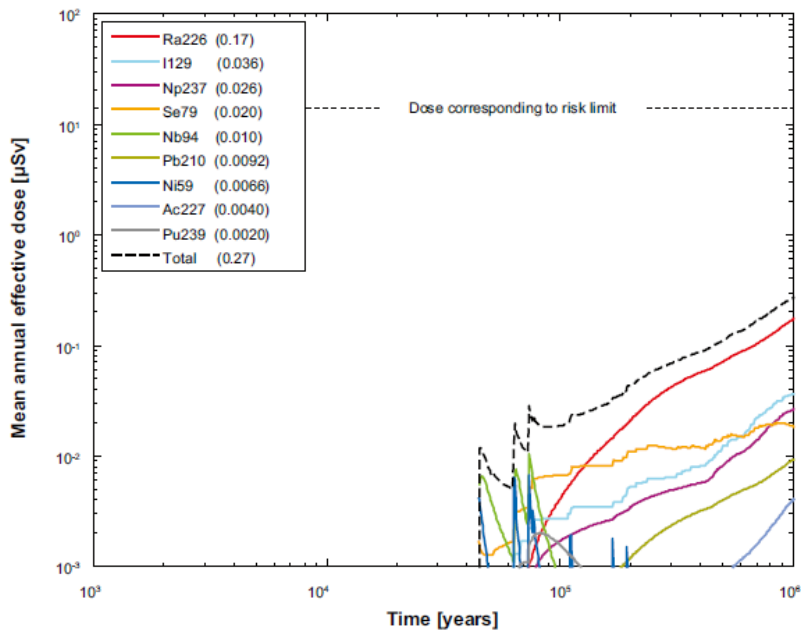
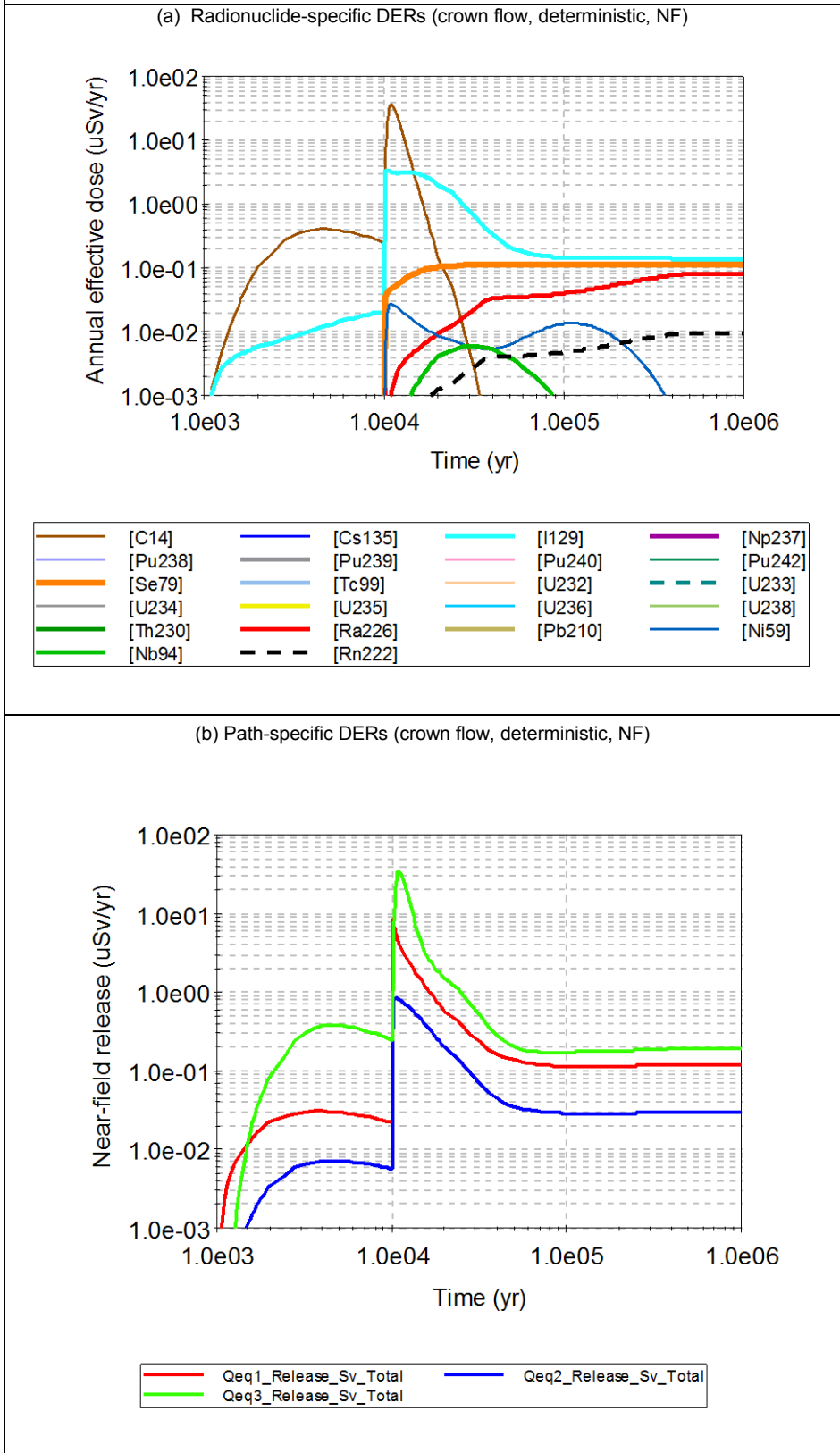
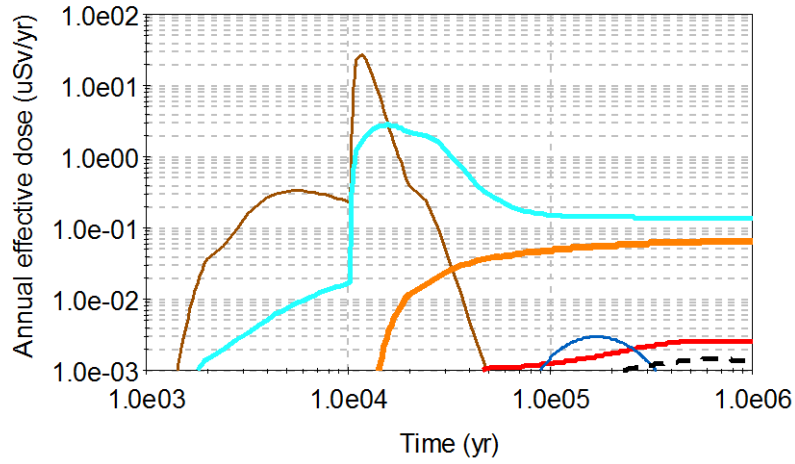


Figure 4-31. Far-field mean annual effective dose for a probabilistic calculation of the central corrosion case, with initial advection in the erosion/corrosion model. The legend is sorted by peak (in the one-million year period) of the mean annual effective dose. The values in brackets are peak dose in units of μSv .

Figure 7: Results of the verification modelling of the Growing Pinhole Failure + Crown Flow scenario with the deposition tunnel-Q3 fracture intersection distance of 5.1 m instead of 118 m for deterministic and probabilistic calculations.

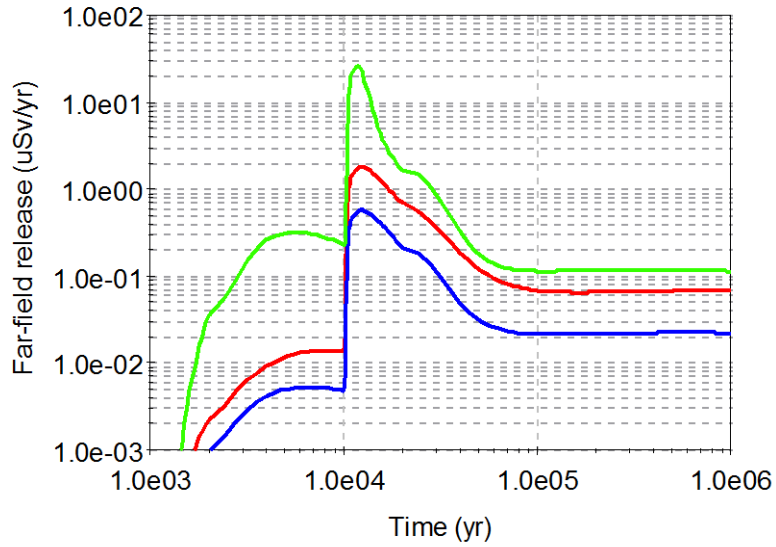


(c) Radionuclide-specific DERs (crown flow, deterministic, FF)



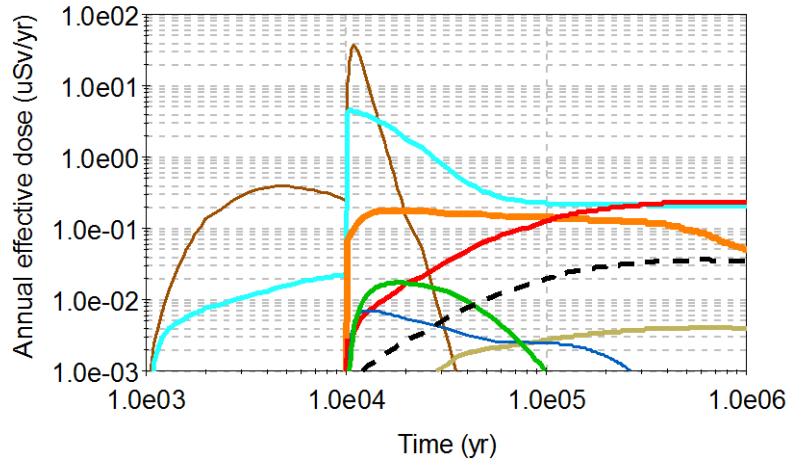
[C14]	[Cs135]	[I129]	[Np237]
[Pu238]	[Pu239]	[Pu240]	[Pu242]
[Se79]	[Tc99]	[U232]	[U233]
[U234]	[U235]	[U236]	[U238]
[Th230]	[Ra226]	[Pb210]	[Ni59]
[Nb94]	[Rn222]		

(d) Path-specific DERs (crown flow, deterministic, FF)



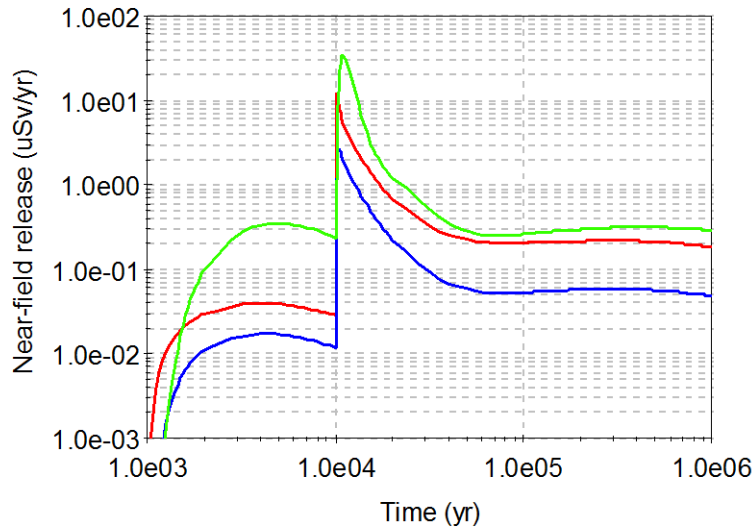
FF_Release_Q1_Sv_Total	FF_Release_Q2_Sv_Total
FF_Release_Q3_Sv_Total	

(e) Radionuclide-specific DERs (crown flow, probabilistic, NF)



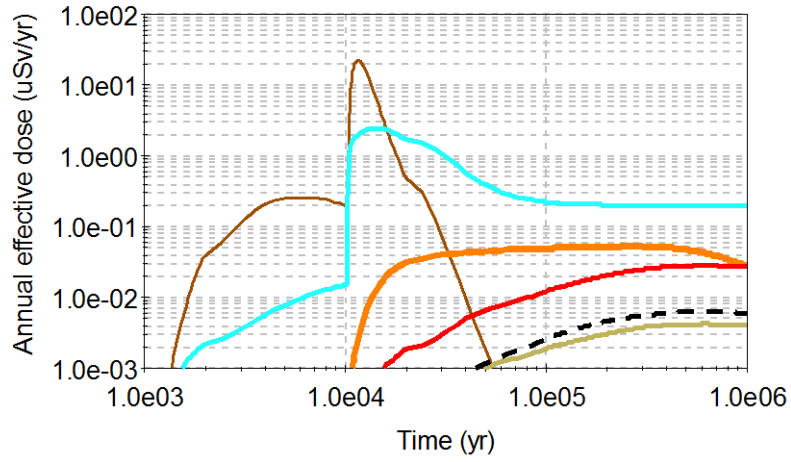
[C14]	[Cs135]	[I129]	[Np237]
[Pu238]	[Pu239]	[Pu240]	[Pu242]
[Se79]	[Tc99]	[U232]	[U233]
[U234]	[U235]	[U236]	[U238]
[Th230]	[Ra226]	[Pb210]	[Ni59]
[Nb94]	[Rn222]		

(f) Path-specific DERs (crown flow, probabilistic, NF)



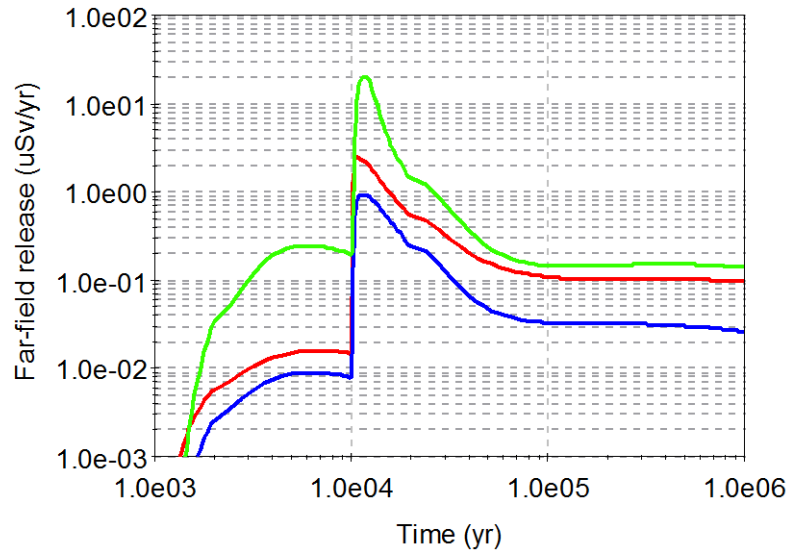
Qeq1_Release_Sv_Total	Qeq2_Release_Sv_Total
Qeq3_Release_Sv_Total	

(g) Radionuclide-specific DERs (crown flow, probabilistic, FF)



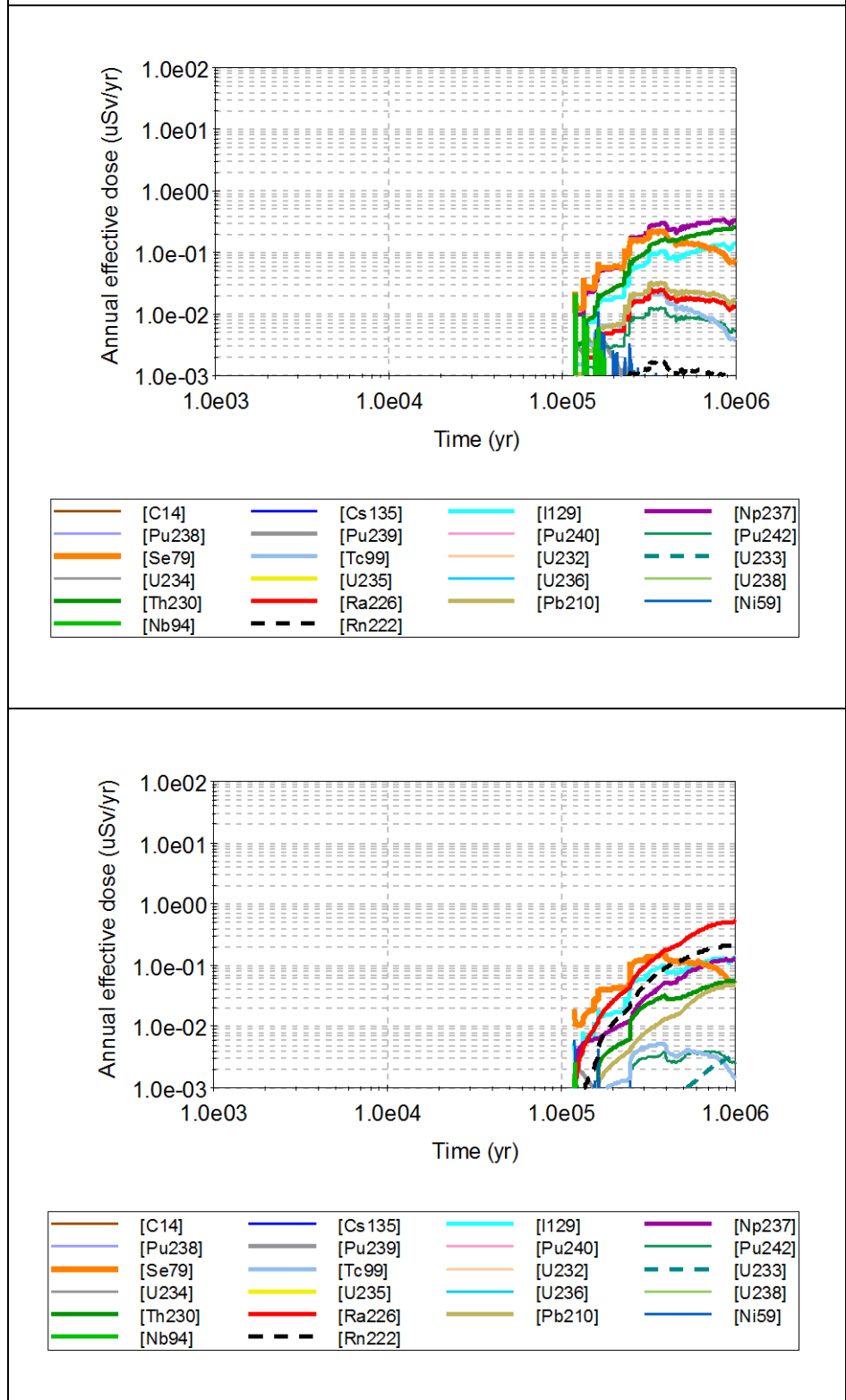
[C14]	[Cs135]	[I129]	[Np237]
[Pu238]	[Pu239]	[Pu240]	[Pu242]
[Se79]	[Tc99]	[U232]	[U233]
[U234]	[U235]	[U236]	[U238]
[Th230]	[Ra226]	[Pb210]	[Ni59]
[Nb94]	[Rn222]		

(h) Path-specific DERs (crown flow, probabilistic, FF)



FF_Release_Q1_Sv_Total	FF_Release_Q2_Sv_Total
FF_Release_Q3_Sv_Total	

Figure 8: Results of probabilistic modelling the corrosion scenario with fast SNF degradation (i.e., faster than the nominal case value of 1×10^{-7} /yr by an order or magnitude): (a) near field, (b) far field.





2014:33

The Swedish Radiation Safety Authority has a comprehensive responsibility to ensure that society is safe from the effects of radiation. The Authority works to achieve radiation safety in a number of areas: nuclear power, medical care as well as commercial products and services. The Authority also works to achieve protection from natural radiation and to increase the level of radiation safety internationally.

The Swedish Radiation Safety Authority works proactively and preventively to protect people and the environment from the harmful effects of radiation, now and in the future. The Authority issues regulations and supervises compliance, while also supporting research, providing training and information, and issuing advice. Often, activities involving radiation require licences issued by the Authority. The Swedish Radiation Safety Authority maintains emergency preparedness around the clock with the aim of limiting the aftermath of radiation accidents and the unintentional spreading of radioactive substances. The Authority participates in international co-operation in order to promote radiation safety and finances projects aiming to raise the level of radiation safety in certain Eastern European countries.

The Authority reports to the Ministry of the Environment and has around 315 employees with competencies in the fields of engineering, natural and behavioural sciences, law, economics and communications. We have received quality, environmental and working environment certification.

Strålsäkerhetsmyndigheten
Swedish Radiation Safety Authority

SE-171 16 Stockholm
Solna strandväg 96

Tel: +46 8 799 40 00
Fax: +46 8 799 40 10

E-mail: registrator@ssm.se
Web: stralsakerhetsmyndigheten.se